THE JOURNAL OF BIOLOGICAL CHEMISTRY VOL. 287, NO. 34, pp. 28986–29002, August 17, 2012

A Novel Dominant Hyperekplexia Mutation Y705C Alters Trafficking and Biochemical Properties of the Presynaptic Glycine Transporter GlyT2*

Received for publication, October 31, 2011, and in revised form, June 18, 2012 Published, JBC Papers in Press, June 29, 2012, DOI 10.1074/jbc.M111.319244

Cecilio Giménez[‡§¶], Gonzalo Pérez-Siles[‡§], Jaime Martínez-Villarreal[‡§¶], Esther Arribas-González[‡¶], Esperanza Jiménez[‡§¶], Enrique Núñez[‡§¶], Jaime de Juan-Sanz[‡§¶], Enrique Fernández-Sánchez[‡], Noemí García-Tardón[‡§¶], Ignacio Ibáñez[‡], Valeria Romanelli[§‖], Julián Nevado[§‖], Victoria M. James[**], Maya Topf[‡‡], Seo-Kyung Chung[§§], Rhys H. Thomas[§§], Lourdes R. Desviat[‡], Carmen Aragón[‡§¶], Francisco Zafra[‡§¶], Mark I. Rees[§§], Pablo Lapunzina[§‖], Robert J. Harvey[**], and Beatriz López-Corcuera[‡§¶1]

From the [‡]Departamento de Biología Molecular and Centro de Biología Molecular "Severo Ochoa," (Consejo Superior de Investigaciones Científicas-Universidad Autónoma de Madrid), Madrid 28049, Spain, the [§]Centro de Investigación Biomédica en Red de Enfermedades Raras, Instituto de Salud Carlos III, Madrid 28029, Spain, the [¶]IdiPAZ-Hospital Universitario La Paz, the [‖]Instituto de Genética Médica y Molecular, IdiPAZ-Hospital Universitario La Paz, Universidad Autónoma de Madrid, Madrid 28046, Spain, the [**]Department of Pharmacology, University College London School of Pharmacy, London WC1N 1AX, United Kingdom, the [‡‡]Institute of Structural and Molecular Biology, Crystallography, Birkbeck College, London WC1E 7HX, United Kingdom, and the [§§]Institute of Life Science, College of Medicine, Swansea University, Swansea SA2 8PP, United Kingdom

Background: Hyperekplexia or startle disease is caused by defects in glycinergic transmission.
Results: A new mutation pY705C in the glycine transporter GlyT2 alters protein trafficking and H^+ and Zn^{2+} transport modulation.
Conclusion: Multiple pathogenic mechanisms may contribute to the complex phenotype of individuals with the Y705C mutation.
Significance: This is the first common dominant mutation associated with hyperekplexia affecting the presynaptic glycine transporter GlyT2.

Hyperekplexia or startle disease is characterized by an exaggerated startle response, evoked by tactile or auditory stimuli, producing hypertonia and apnea episodes. Although rare, this orphan disorder can have serious consequences, including sudden infant death. Dominant and recessive mutations in the human glycine receptor (GlyR) α1 gene (*GLRA1*) are the major cause of this disorder. However, recessive mutations in the presynaptic Na^+/Cl^--dependent glycine transporter GlyT2 gene (*SLC6A5*) are rapidly emerging as a second major cause of startle disease. In this study, systematic DNA sequencing of *SLC6A5* revealed a new dominant GlyT2 mutation: pY705C (c.2114A→G) in transmembrane domain 11, in eight individuals from Spain and the United Kingdom. Curiously, individuals harboring this mutation show significant variation in clinical presentation. In addition to classical hyperekplexia symptoms, some individuals had abnormal respiration, facial dysmorphism, delayed motor development, or intellectual disability. We functionally characterized this mutation using molecular modeling, electrophysiology, [^{3}H]glycine transport, cell surface expression, and cysteine labeling assays. We found that the introduced cysteine interacts with the cysteine pair Cys-311–Cys-320 in the second external loop of GlyT2. This interaction impairs transporter maturation through the secretory pathway, reduces surface expression, and inhibits transport function. Additionally, Y705C presents altered H^+ and Zn^{2+} dependence of glycine transport that may affect the function of glycinergic neurotransmission *in vivo*.

The extracellular concentration of synaptic glycine is regulated by Na^+/Cl^--dependent glycine transporters. These proteins mediate reuptake of glycine into presynaptic terminals (GlyT2)[2] and glial cells adjacent to glycinergic inhibitory neurons (GlyT1) (1). Mouse knock-out studies have revealed that glial GlyT1 is the main regulator of the extracellular glycine concentrations (2). By contrast, neuronal GlyT2 is involved in the removal and recycling of synaptic glycine generating a vectorial flow from the synaptic cleft into the terminal, supplying substrate to the low affinity vesicular inhibitory amino acid transporter (2, 3). Inactivation of the GlyT2 gene (*Slc6a5*) pre-

* This work was supported by Spanish Dirección General de Enseñanza Superior e Investigación Científica Grants BFU2005-05931/BMC and BIO2005-05786, Ministerio de Ciencia e Innovación Grant SAF2008-05436, Comunidad Autónoma de Madrid Grants 11/BCB/010 and S-SAL-0253/2006, Ministerio de Economia y Competitividad Grant SAF2011-28674, Centro de Investigación Biomédica en Red de Enfermedades Raras Intramural Project U-751/U-753, an institutional grant from the Fundación Ramón Areces, Medical Research Council Grant G0601585, and Action Medical Research Grant 1966. The group is member of the European Regional Development Fund Grant BFU2007-30688-E/BFI.

[1] To whom correspondence should be addressed: Dept. de Biología Molecular, Centro de Biología Molecular "Severo Ochoa," Universidad Autónoma de Madrid, 28049 Madrid, Spain. Tel.: 34-91-1964631; Fax: 34-91-1964420; E-mail: blopez@cbm.uam.es.

[2] The abbreviations used are: GlyT, glycine transporter; GlyR, glycine receptor; GLR, glycine receptor subunit; HBS, Hepes-buffered saline; $LeuT_{Aa}$, leucine transporter from *A. aeolicus*; MesNa, sodium methanethiosulfonate; MTSEA, 2 aminoethyl methanethiosulfonate; SLC, solute carrier; TCEP, tris(2-carboxyethyl) phosphine; TM, transmembrane domain; HBS, Hepes-buffered saline; MDCK, Madin-Darby canine kidney.

vents glycine loading into synaptic vesicles, impairing inhibitory glycinergic neurotransmission (4). GlyT2 knock-out mice have a complex motor phenotype (4, 5) that mimics clinical signs of hyperekplexia or startle disease (OMIM 149400). This rare human disorder is characterized by an exaggerated startle response to acoustic or tactile stimuli (6). Startle disease can have serious consequences for neonates, including brain damage and/or sudden death caused by apnea episodes. The abnormal startle response, which can provoke unprotected falls resulting in injury, can persist throughout development and into adulthood (7). However, unlike rodent, cattle, and canine defects (6), humans with *SLC6A5* mutations survive, and clinical signs often resolve after the neonatal and infantile risk period (8).

Genetic analysis of individuals with human hyperekplexia has revealed mutations in genes for postsynaptic proteins involved in glycinergic neurotransmission. These include the GlyR α1 and β subunits (*GLRA1* and *GLRB*) and proteins that assist receptor trafficking to the synaptic membrane (9–11). Sequencing the 16 exons of the human GlyT2 gene (*SLC6A5*) also revealed that missense, nonsense, and frameshift mutations affecting presynaptic glycine transport can cause hyperekplexia (8, 12). The structure of a prokaryotic homologue ($LeuT_{Aa}$) of the SLC6 family (13) has provided a useful model for explaining the effects of selected missense mutations on Na^+ and glycine-binding residues crucial for transport activity (6, 8, 12). It is also noteworthy that the majority of GlyT2 mutations were recessive, producing bi-allelic loss of function caused by the absence of protein in the plasma membrane or by production of an inactive transporter (6). In the present study, we report the identification of a novel dominant mutation (c.2114A→G, pY705C) in exon 15 of *SLC6A5*. This change was found in eight individuals from three families in two cohorts of hyperekplexia patients that were devoid of GlyR gene mutations. Functional characterization of this GlyT2 substitution revealed the introduced cysteine impacts on transporter protein maturation through the secretory pathway and alters the H^+ and Zn^{2+} dependence of glycine transport. The biochemical features of the mutant transporter may produce detrimental effects on glycinergic inhibition *in vivo*.

EXPERIMENTAL PROCEDURES

Molecular Genetic Analysis of the Human GlyT2 Gene (SLC6A5)—Informed consent was obtained from all individuals using guidelines approved by the local ethical committees. Patients of both sexes were studied. Patient genomic DNA was amplified using primers for the 16 exons of the *SLC6A5* gene as previously described (8). 60 ng of genomic DNA were amplified using an Expand high fidelity PCR system (Roche Applied Science) in 25-μl reactions containing 10 pmol of each primer, 1× buffer with 1.5 mM $MgCl_2$, 200 μM dNTPs, and 1 unit of Taq polymerase (Roche Applied Science). PCR conditions were 94 °C for 5 min followed by 35 cycles of 30 s at 94 °C, 30 s at 60 °C, and 30 s at 72 °C. Amplification products were analyzed on 2% agarose gels, extracted with a QIAQuick gel extraction kit (Qiagen), and sequenced employing BigDye Terminator v.3.1 mix (Applied Biosystems Foster City, CA). Genomic DNA from 200 commercially available controls was obtained from the European Collection of Cell Cultures, human random control. Population analysis was conducted by DNA sequencing of control amplicons or using the artificially created restriction site method (14), where an NdeI site is introduced into control but not mutated amplicons during PCR. Electropherograms were analyzed using Sequencher (Gene Codes Corp., Ann Arbor, MI). Analysis of copy number variations in hyperekplexia genes was assessed by multiplex ligation-dependent probe amplification. Briefly, DNA (250 μg) was tested using the SALSA multiplex ligation-dependent probe amplification kit P274 (MRC Holland), which evaluates several regions of *GLRA1*, *GLRB*, and *SLC6A5*. No abnormalities (deletions nor duplications) were observed in any of the samples evaluated, ruling out copy number variations as a cause of hyperekplexia in these cases.

In Silico Analysis—Conservation of the mutated residues was assessed by alignment of orthologous and human protein sequences using ClustalW software (15). The putatively damaging effects of the predicted amino acid substitution was assessed using the PolyPhen-2 program (16) that gives the results as "benign," "possibly damaging," "probably damaging," or "unknown." A GlyT2 homology model was obtained using MODELLER (17) as previously reported (6, 18), based on the crystal structure of $LeuT_{Aa}$ from the bacterium *Aquifex aeolicus* (Protein Data Bank code 2A65) (13).

Mutagenesis and Expression of Human GlyT2 cDNA in Mammalian Cells—The human GlyT2 cDNA was cloned into the vectors pRC-CMV (Invitrogen) and pEGFP-C1 (Clontech) as previously described (8). Missense mutations were generated in pRC-CMV GlyT2 by site-directed mutagenesis using the QuikChange kit (Stratagene). Two independent *Escherichia coli* colonies carrying the mutant plasmids were characterized by DNA sequencing and [^{3}H]glycine transport activity. We sequenced the full coding region of each construct to verify that only the desired mutation had been introduced. Transient expression in COS7 cells was performed as described (18) using Lipofectamine Plus (Invitrogen) or Neofectin™ (MidAtlantic Biolabs). The cells were incubated for 48 h at 37 °C, unless otherwise indicated in the figure legends. For electrophysiological recordings, the human GlyT2 cDNA was subcloned into the vector pSP64T, generously provided by Dr. Carmen Montiel (Universidad Autónoma of Madrid, Madrid, Spain).

Glycine Transport Assays—Transport assays in COS7 cells were performed at 37 °C in 0.25 ml of Hepes-buffered saline (HBS: 150 mM NaCl, 10 mM Hepes-Tris, pH 7.4, 1 mM $CaCl_2$, 5 mM KCl, 1 mM $MgSO_4$, 10 mM glucose). 2 μCi/ml [^{3}H]glycine (1.6 TBq/mmol; PerkinElmer Life Sciences) isotopically diluted at 10 μM final glycine concentration was used (19), unless a different concentration is specified. The reactions were terminated after 10 min by aspiration followed by washing with HBS. Transport was measured by subtracting the glycine accumulation by mock-transfected COS7 cells from that of GlyT2 transfected cells and normalizing to the protein concentration. Kinetic analysis was performed by varying glycine concentration in the uptake medium between 10 and 1000 μM.

Expression of the Human GlyT2 cDNA in Xenopus Oocytes—Wild-type and mutant GlyT2 cDNAs were cloned in the vector pSP64T, which contains a β1-globin promoter. Constructs

were linearized with XbaI, and cRNA was transcribed with SP6 polymerase and capped with 5′7-methylguanosine using the mMESSAGE mMACHINE SP6 RNA kit (Ambion Inc.). *Xenopus laevis* females were obtained from *Xenopus* Express (France). The oocytes were harvested from *X. laevis* anesthetized in tricaine methasulfonate 0.10% (w/v) solution in tap water. All of the procedures were in accordance with the Spanish and European guidelines for the prevention of cruelty to animals. The follicular membrane was removed by incubation in a medium (90 mM NaCl, 1 mM KCl, 1 mM $MgCl_2$, 5 mM Hepes, pH 7.4) containing 300 units/ml collagenase (Type 1; Sigma) for 1 h. Wild-type or mutant mRNAs (50 ng) were injected into defolliculated stage V and VI *X. laevis* oocytes. The oocytes were maintained in Barth's medium (88 mM NaCl, 1 mM KCl, 0.33 mM $Ca(NO_3)_2$, 0.41 mM $CaCl_2$, 0.82 mM $MgSO_4$, 2.4 mM $NaHCO_3$, and 10 mM Hepes, pH 7.4), and transport or electrophysiological experiments were assayed 5 days post-injection.

Two-microelectrode Voltage-Clamp Recordings from Xenopus Oocytes—Electrophysiological recordings were obtained after incubation of the injected oocytes at 18 °C in standard oocyte solution (100 mM NaCl, 2 mM KCl, 1 mM $CaCl_2$, 1 mM $MgCl_2$, 10 mM Hepes, pH adjusted to pH 7.5 with HCl). Two-electrode voltage clamp was used to measure and control the membrane potential and to monitor the capacitative currents using Axoclamp 900A (Axon Instruments), digitized using a Digidata 1440 (Axon Instruments). Both instruments were controlled by pCLAMP software (Axon Instruments), and the results were analyzed using Clampfit 10.2 software (Axon Instruments). Recordings were performed at room temperature using standard micropipettes filled with 3 M KCl (resistance varied between 0.5 and 2 MΩ). The oocytes were held at −40 mV, and to obtain current-voltage (I-V) relations, the pulse protocol consisted of 350-ms voltage steps between −130 and +50 mV in 20 mV steps. The currents were subjected to low pass filtering at 100 Hz.

Cell Surface Labeling—Thiol-specific biotinylation and total surface biotinylation was performed with MTSEA-biotin (Toronto Research Chemicals Inc., Toronto, Canada) and sulfo-NHS-SS-biotin (Pierce) on transfected COS7 cells as described (20, 21). 0.5 mM MTSEA-biotin or 1.5 mg/ml sulfo-NHS-SS-biotin and a 3-h incubation with streptavidin-agarose beads (Sigma) were used. Biotinylated proteins (B) were eluted from the beads with Laemmli buffer (40 mM Tris, pH 6.8, 2% SDS, 10% glycerol, 0.1 M DTT, 0.01% bromphenol blue) for 10 min at 70 °C and then analyzed in Western blots (7.5% SDS-PAGE) with anti-GlyT2 antibody (Santa Cruz). Protein bands were visualized by ECL and quantified on a GS-710 calibrated imaging densitometer from Bio-Rad with Quantity One software, using film exposures in the linear range. Loading controls were performed by reprobing Western blot membranes using an anti-calnexin antibody. Standard errors were calculated from at least three separate experiments.

GlyT2 Subcellular Localization—Wild-type or mutant GlyT2 in pEGFP-C1 were transfected in MDCK cells and 48 h later were subjected to immunofluorescence as described previously (22) using the antibody against the indicated marker protein. Secondary antibodies were coupled to Alexa Fluor® 555. Alternatively, the cells were transfected with pEGFP-C1 GlyT2 (23) and were fixed with 4% paraformaldehyde in PBS. The cells were visualized by confocal microscopy on a LSM510 confocal microscope (Zeiss) using a vertical microscope Axio Imager.Z1 M (Zeiss).

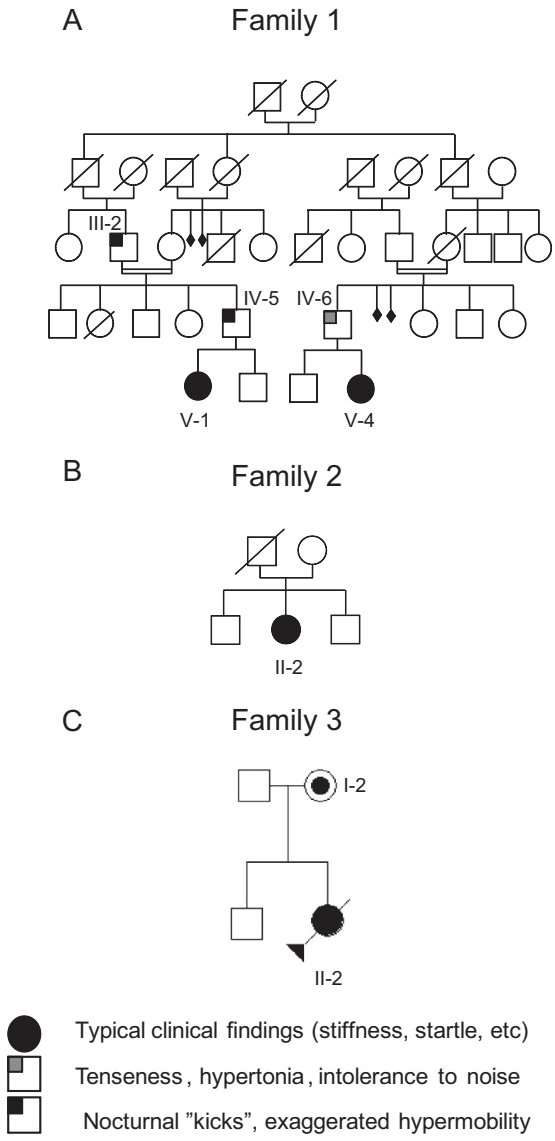

FIGURE 1. **Pedigree of families 1 (*A*), 2 (*B*), and 3 (*C*).** Individuals are numbered according to their position in the pedigree lines as I, II, III, and IV, and then each individual from left to right as 1, 2, 3, etc. Males and females are represented by *squares* and *circles*, respectively. *Shaded symbols* represent individuals with the Y705C mutation or who are/were affected, with clinical signs observed.

RESULTS

Patient Information—A total of 16 probands from Spain and 188 from the UK with clinical diagnosis of hyperekplexia, all of which had proved gene-negative in screens of *GLRA1* and *GLRB*, were provided from neurological units. Genomic DNA samples from the patients were screened for *SLC6A5* mutations. Clinical features of patients carrying the novel mutation in the *SLC6A5* gene are summarized below. Fig. 1 shows the pedigrees of the patient families.

The first patient from family 1, V-1, displayed perinatal onset persistent crying and hypertonia. This was ameliorated when she was removed from the neonatal intensive care unit and was placed in a quiet, low stimuli environment. Physical examination at day 7 revealed an exaggerated startle reaction and prominent head retraction. She had delayed motor development and showed a severe degree of intellectual disability. With the second patient from family 1, V-4, concern was raised when the child was 1 month old because of hypertonia and abnormal crying. Neurological evaluation demonstrated abnormal head retraction and hypertonia, which improved during sleep. Patient IV-5 from family 1 had similar neonatal behavior to V-1; he "kicked" and had exaggerated movements during rest at bed, mainly when sleeping. Patient IV-6 in family 1 showed some intolerance to noise and crowded places, and when he was a boy suffered from attacks of stiffness precipitated by surprise or school tests.

Patient II-2 in family 2 was a girl who presented with stiffness and frequent falling and was intellectually intact. Patient II-2 in family 3 had perinatal hypertonia with clonus (variable, partially resolving in sleep) and triggered startle episodes (paroxysmal clonic movements). In addition she had abnormal respiration with prominent apnea episodes. Physically she had several dysmorphic features: tongue protrusion, striking excess neck skin folds, large atrial-septal defect, short palpebral fissures, small carp-like mouth, subtly low set ears, single palmar crease, contractures at the knees, and overlapping clenched fingers and hands. Cranial calcification was also seen. Her MRI demonstrated small focal areas of signal change in the deep, subcortical white matter of both cerebral hemispheres and possible gyral swelling. She died aged 21 weeks having spent the majority of her life in pediatric intensive care. The mother is apparently asymptomatic. She was physically examined at the age of thirty-one and no abnormality or excessive startle was detected.

Genetic Analysis—Genomic DNA samples from 204 individuals with hyperekplexia who had tested negative for disease-causing mutations in *GLRA1* (5q33.1) and *GLRB* (4q32.1) were scanned on all 16 coding exons and extended flanking intronic regions of *SLC6A5* (11p15.1), encoding human GlyT2. Several single-nucleotide polymorphisms present in patients and controls were found. In addition, DNA sequence analysis revealed a heterozygous nonsynonymous change (c.2114A→G) in exon 15 in four of the patients analyzed (patients V-1 and V-2 of family 1, patient II-2 of family 2, and patient II-2 of family 3). Familial analysis revealed the presence of this sequence variant in four more individuals (Fig. 1). This change was not detected in 600 unrelated, normal control chromosomes (data from the United Kingdom; not detected in 400 normal control chromosomes, Caucasian samples), as assessed using two different techniques (see "Experimental Procedures"). This mutation resulted in a tyrosine (T*A*T) to cysteine (T*G*T) substitution at position 705 (pY705C) in transmembrane domain 11 (TM11; Fig. 2). Homology modeling of GlyT2 using the crystal structure of the $LeuT_{Aa}$ (13) located Tyr-705 at the carboxyl-terminal portion of the TM11, near the extracellular face of the transporter (Fig. 2*B*). A loss of a hydrogen bond with the side chain of Glu-701 is predicted. Phylogenetic comparisons of the TM11 region of GlyT2 show high evolutionary conservation of Tyr-705 (Fig. 2*C*). Alignment of GlyT2 with other Na^+/Cl^--dependent neurotransmitter transporters of the SLC6 family demonstrates that a tyrosine is found at the equivalent position in most human neurotransmitter transporters from the GABA, amino acid, and monoamine subfamilies (norepinephrine transporter and dopamine transporter) with the exception of GABA transporter 1 and serotonin transporter (Fig. 2*D*). This suggests that Tyr-705 has a relevant role for transporter function within this superfamily and accordingly, the Y705C substitution was predicted to be "probably damaging" in PolyPhen-2 analysis, with a score of 1.000.

Mutagenesis and Functional Characterization—Functional consequences of the Y705C mutation were initially assessed by assaying [^{3}H]glycine uptake of recombinant wild-type and mutant GlyT2 after transient expression in COS7 cells (Fig. 3*A*). The V_{max} of glycine transport by the Y705C mutant was reduced to ~60% as compared with wild-type GlyT2 (23 ± 2.5 for the Y705C *versus* 38 ± 3.2 nmol of Gly/mg of protein/5 min for wild type). The co-expression of wild-type and Y705C transporters resulted in a V_{max} of 30 ± 3.1 nmol of Gly/mg of protein/5 min, representing 79% of wild-type GlyT2. This value is close to the predicted average value of the activity of each transporter population. A slight but significant increase of the K_m for glycine was observed in the Y705C mutant when expressed alone. Investigation of other features of glycine transport by GlyT2 indicated that sensitivity to Na^+ and Cl^-, the ions required for transport, was unaffected in Y705C mutant, and the sensitivity of the mutant transporter to the inhibition by the selective GlyT2 inhibitor ALX1393 was unchanged as compared with wild-type GlyT2 (data not shown).

Additional functional characterization was performed by overexpressing wild-type and mutant GlyT2 in *Xenopus* oocytes to examine the electrophysiological properties of both proteins. As shown in Fig. 3*B*, glycine-induced inward currents were observed in oocytes expressing either wild-type GlyT2 or the Y705C mutant. In agreement with the reduced V_{max} for glycine transport observed in COS cells, maximal currents recorded from oocytes were ~35% lower than observed for wild-type GlyT2. We also studied the voltage dependence of the observed currents by employing a voltage-clamp protocol consisting of long square pulses from −130 to +50 mV. The current triggered by glycine showed inward rectification for both transporters (Fig. 3*C*). The *I-V* relationships were similar in shape, suggesting no alteration of the voltage dependence of glycine transport. However, at each voltage examined, the current mediated by wild-type GlyT2 was larger than that of the Y705C mutant.

Plasma Membrane Expression—One possible explanation for the reduction in V_{max} for glycine transport of the Y705C mutant could be impaired plasma membrane expression. We determined the levels of transporters present in the plasma membrane using two different approaches. First, we expressed EGFP-tagged wild-type GlyT2 or the Y705C mutant in MDCK cells (Fig. 4*A*), immunolabeling the cells for the plasma membrane marker protein E-cadherin (22, 24). The percentage of Y705C co-localization with the plasma membrane marker was

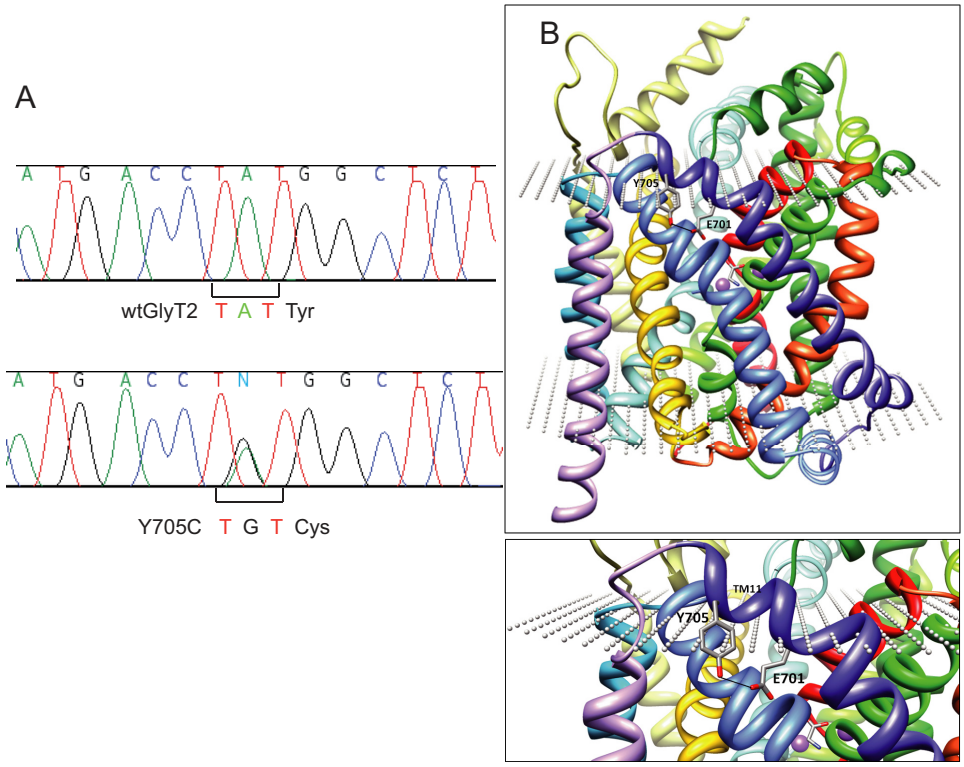

C

Homo sapiens	VCWAFVTPTILTFILCFSFYQWEPMTYGSYRYPNWSMVLGWLMLACSVIWIP
Mus musculus	VCWAFVTPTILTFILCFSFYQWEPMTYGSYRYPNWSMVLGWLMLACSVIWIP
Rattus norvegicus	VCWAFVTPTILTFILCFSFYQWEPMTYGSYRYPNWSMVLGWLMLACSVIWIP
Canis familiaris	VCWAFVTPTILTFILCFSFYQWEPMTYGSYRYPNWSMVLGWLMLACSVIWIP
Monodelphis domestica	VCWAFVTPTILTFILCFSFYQWEPMTYGSYRYPNWSMVLGWLMLACSVIWIP
Gallus gallus	VCWAFVTPTILTFILCFSFYQWEPMTYGAYHYPGWSMVLGWLMLACSVIWIP
Danio rerio	VCWAFVTPTILTFILALSLYQWKVMTYEDYTYPNWSMVLGWLMVICSVIWIP
Strongylocentrotus p.	VNWSAFTPGLMVFVLFFNWLQWVEPSYNG-PFPTWAVIIGWLMTTMSLIWIP

D

hGlyT2	SLC6A5	CWAFVTPTILTFILCFSFYQWEPMTYGS-YRYPNWSMVLGWLMLACSVIWIP
hGlyT1	SLC6A9	CWRFVSPAIIFFILVFTVIQYQPITYNH-YQYPGWAVAIGFLMALSSVLCIP
hPROT	SLC6A7	CWLFLSPATLLALMVYSIVKYQPSEYGS-YRFPPWAELLGILMGLLSCLMIP
hTAUT	SLC6A6	SWAVITPVLCVGCFIFSLVKYVPLTYNKTYVYPNWAIGLGWSLALSSMLCVP
hGAT1	SLC6A1	CWSFFTPIIVAGVFIFSAVQMTPLTMGN-YVFPKWGQGVGWLMALSSMVLIP
hGAT2	SLC6A13	CWLFLTPAVCTATFLFSLIKYTPLTYNKKYTYPWWGDALGWLLALSSMVCIP
hGAT3	SLC6A11	CWMIMTPGICAGIFIFFLIKYKPLKYNNIYTYPAWGYGIGWLMALSSMLCIP
hBGT1	SLC6A12	SWLFLTPGLCLATFLFSLSKYTPLKYNNVYVYPPWGYSIGWFLALSSMVCVP
hCRTR	SLC6A8	CWSFFTPLVCMGIFIFNVVYYEPLVYNNTYVYPWWGEAMGWAFALSSMLCVP
hNET	SLC6A2	CWKFVSPAFLLFVVVVSIINFKPLTYDD-YIFPPWANWVGWGIALSSMVLVP
hDAT	SLC6A3	CWKLVSPCFLLFVVVVSIVTFRPPHYGA-YIFPDWANALGWVIATSSMAMVP
hSERT	SLC6A4	CWVAISPLFLLFIICSFLMSPPQLRLFQ-YNYPYWSIILGYCIGTSSFICIP

FIGURE 2. **Genetic and structural analysis of the Y705C mutant.** *A*, partial sequences of exon 15 from control and patient 1 DNAs, respectively. Note the heterozygous single-nucleotide polymorphism c.2114A→G changes the codon TAT to TGT, resulting in a pY705C substitution in GlyT2. *B*, molecular model of GlyT2 showing the localization of Tyr-705 in TM11. *C*, phylogenetic comparison of TM11 regions of GlyT2 containing the amino acid Tyr-705 (in *red*). *D*, sequence alignment of GlyT2 TM11 region in human SLC6 family members. Sequences were obtained from NCBI (www.ncbi.nlm.nih.gov) and were aligned using ClustalW software and MUSCLE alignment server.

76.8 ± 2.3% compared with wild-type GlyT2. In addition, surface labeling with the nonpermeant reagent Sulfo-NHS-SS-biotin of the proteins expressed in the plasma membrane of COS7 cells allowed the isolation and quantification of the surface-resident transporters. In agreement with this finding, the Y705C mutant amounted for 68.9 ± 5.7% of wild-type GlyT2 levels (Fig. 4*B*). GlyT2 protein expressed in cultured cells appears as a mature 100-kDa protein band, which is the form present on the plasma membrane, and a 75-kDa underglycosylated immature transporter (25). As shown in Fig. 4*B*, the Y705C mutant showed a higher proportion of immature precursor compared with wild-type GlyT2, so that the mature/immature protein ratio was 50% reduced for the mutant. This is highly suggestive of a deficiency in the biogenesis and processing of the Y705C mutant along the secretory pathway, slowing the transformation of the immature precursor into the mature protein. However, we did not observe clear co-localization of the transporter mutant with the endoplasmic reticulum marker (calnexin), nor with other cellular markers such as TGN38, Rab5, or the early endosome marker EEA1 as compared with wild-type GlyT2 (Fig. 4*C*). This suggests that the mutant protein is not arrested in a precise compartment of the secretory pathway but perhaps progresses slowly along the endomembrane system. In addition, no alteration of the typical GlyT2

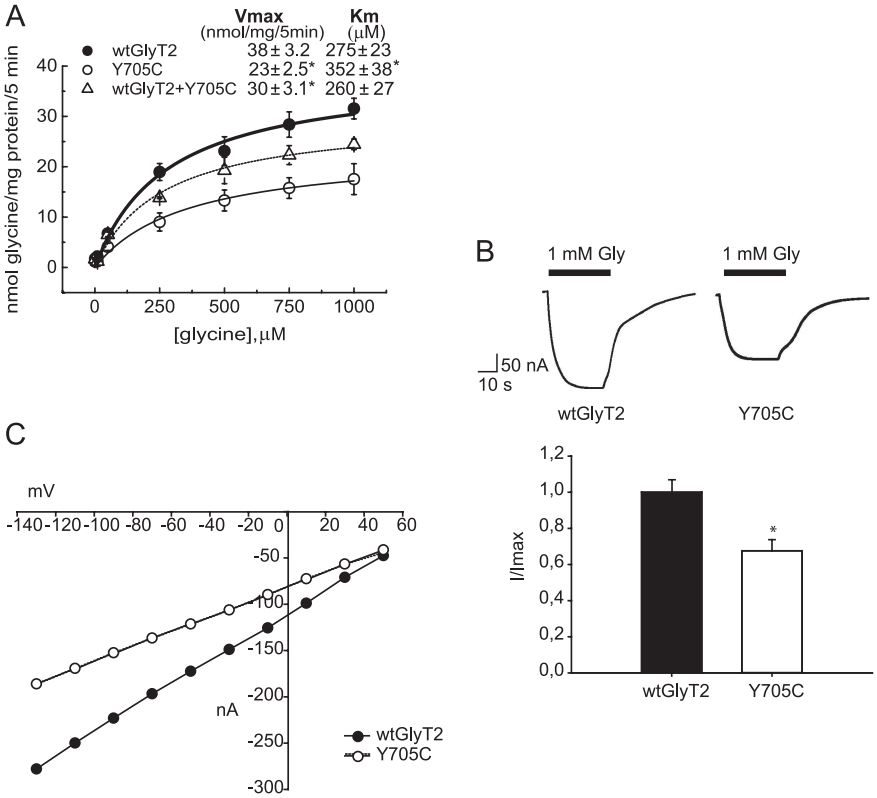

FIGURE 3. **Glycine transport and electrophysiological characterization of wild-type GlyT2 and the Y705C mutant.** *A*, COS7 cells expressing the indicated transporters were assayed for ^{3}[H]glycine transport during 10 min in HBS containing 150 mM NaCl in the presence of increasing glycine concentrations from 0.5 to 1 mM. Experimental data were fitted to hyperbolae. Kinetic parameters are indicated on the graph. *, significantly different from wild-type GlyT2, $p < 0.05$ in Student's *t* test. *B*, inward currents evoked by glycine in representative oocytes expressing wild-type GlyT2 or the Y705C mutant. The cells were voltage-clamped at −40 mV, and 1 mM glycine was superfused for the period indicated by the *solid bar*. Histogram represents arithmetic means ± S.E. ($n = 5$–10 oocytes) of normalized inward currents for wild-type GlyT2 and the Y705C mutant. *, significantly different from wild-type GlyT2, $p < 0.05$ in Student's *t* test. *C*, current-voltage plots of the glycine-mediated inward currents of wild-type GlyT2 and Y705C mutant determined by subtracting, in each case, the currents observed in the absence of glycine.

apical sorting (26) was observed in polarized MDCK cells growing in Transwells (Fig. 4*D*), because the asymmetric distribution of the Y705C mutant was coincident with that of wild-type GlyT2.

Substitution Analysis of Tyr-705—Multiple amino acid substitutions at Tyr-705 showed a comparable, although smaller impairment of plasma membrane localization than that observed for Y705C (Fig. 5*A*). This suggests that the defect in transporter biogenesis is not only due to the introduction of Cys-705 but also due to Tyr-705 removal. Moreover, different Tyr-705 substitutions had heterogeneous effects on glycine transport (Fig. 5*B*). Y705F or Y705A had no or low impact, showing 100 ± 12 and 80 ± 10% of wild-type transport, respectively. By contrast, Y705K and Y705S surpassed wild-type activity by 108 ± 11 and 135 ± 10%, respectively. Remarkably, substitution by glutamic acid (Y705E) profoundly impaired function resulting in 37 ± 4% of wild-type transport. Because transport activity of these mutants does not correlate with membrane expression, Tyr-705 substitutions affect the activity of surface transporters in addition to membrane trafficking.

To further investigate the effect of the cysteine substitution found in the hyperekplexia patients and taking into account that this residue can potentially form disulfide bonds with other cysteines, we performed DTT treatment on cells expressing Tyr-705 mutants. Interestingly, DTT rescued the transport activity of the Y705C mutant from 61 ± 6 to 100 ± 7% of wild-type transport (Fig. 5*B*). As expected, this effect was specific for the Y705C mutant, suggesting that glycine transport activity was restored by reduction of a disulfide bond involving Cys-705. DTT can readily cross the plasma membrane and may affect both transporter trafficking and transport activity. To distinguish between these two possibilities, we used the non-permeant reducing agents MesNa (27) and TCEP (28) (Fig. 5, *C* and *D*). Both reagents consistently produced lower recovery of Y705C function than DTT. This suggests the internal access of the reagent is important for the activation. The small activation produced by the negatively charged MesNa might be due to its decreased reactivity compared with the uncharged TCEP. However, none of the nonpermeant reagents reached the activation produced by DTT. We therefore assumed that DTT can improve a defect in the processing/folding of the transporter during biogenesis, whereas MesNa or TCEP can only "activate" plasma membrane-localized Y705C. Consistent with this theory, Fig. 5*D* shows that MesNa and TCEP promoted higher activation of the Y705C mutant than wild-type GlyT2 or the Y705A mutant.

DTT Increases Plasma Membrane Expression of the Y705C Mutant—Next, we wished to know whether DTT activation targets the intracellular Y705C transporter and increases

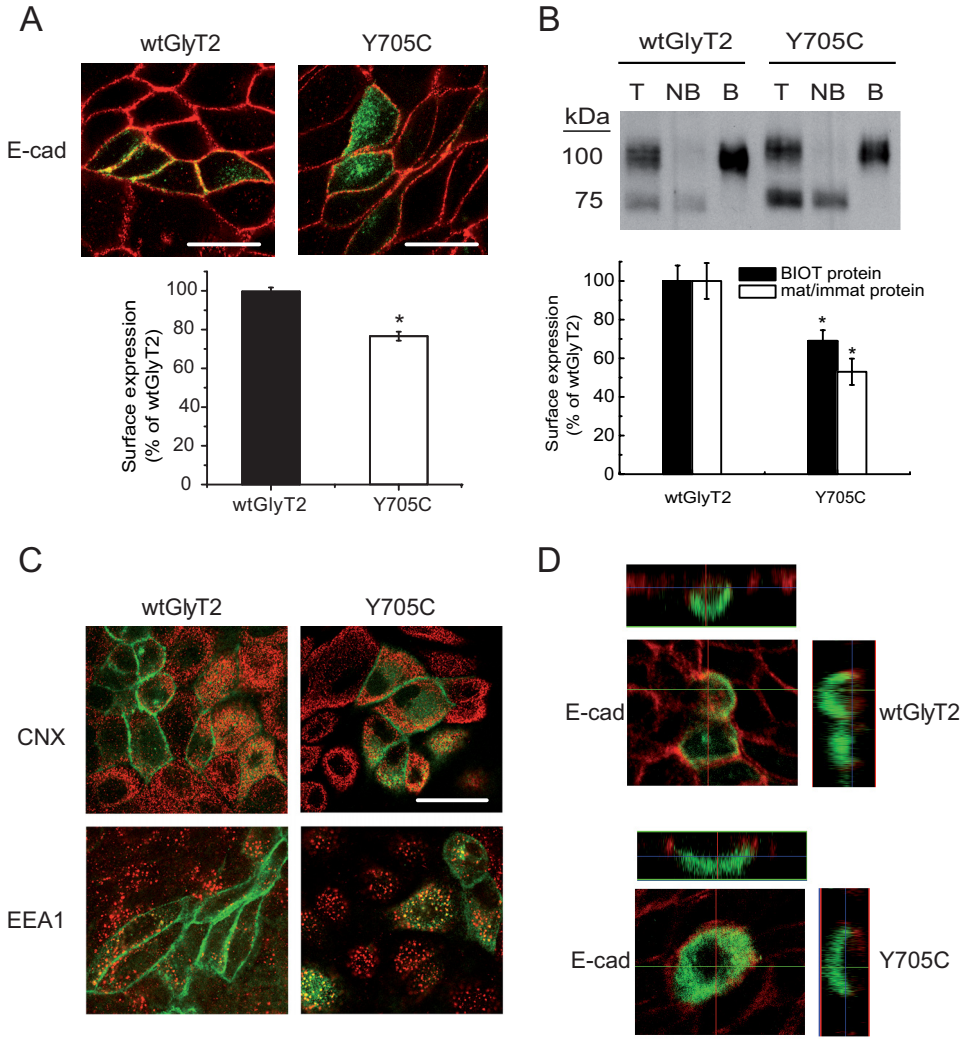

FIGURE 4. **Cell and plasma membrane expression of wild-type GlyT2 and Y705C.** *A*, immunofluorescence quantification of plasma membrane transporters. Wild-type EGFP-tagged GlyT2 or Y705C expressed in MDCK cells for 48 h were immunolabeled for the plasma membrane marker E-cadherin (*E-cad*). Two channel confocal images were obtained (*green* for GlyT2 and *red* for E-cadherin), and regions occupied by E-cadherin were taken as plasma membrane and regions inside the cadherin staining were taken as intracellular, using the Image J ROI manager. After applying an automatic threshold to adjust images, the fluorescence intensity was measured separately for membrane and intracellular regions, and the percentage of transporter in plasma membrane was calculated (histogram). This process was performed at least in 150 cells/condition. *, $p < 0.05$ values calculated using Student's *t* test by comparing wild-type GlyT2 with the Y705C mutant. *B*, COS7 cells expressing wild-type GlyT2 or Y705C mutant were subjected to biotinylation as described under "Experimental Procedures." 8 μg of total (*lanes T*) and nonbiotinylated proteins (*lanes NB*) and 24 μg of biotinylated proteins (*lanes B*) were subjected to Western blotting for GlyT2 detection, and the membranes were reprobed for calnexin immunoreactivity as a loading control. *Lower panel*, densitometric analysis. *Black bars*, total transporter that was biotin-labeled (*B* as a % of *T*) as percentage of that of wild-type GlyT2. *Open bars*, mature/immature transporter ratio (100 kDa/75 kDa) as a percentage of the ratio (100 kDa/75 kDa) for wild-type GlyT2. *, $p < 0.05$ in Student's *t* test. *C*, MDCK cells expressing wild-type EGFP-tagged GlyT2 or Y705C were immunolabeled for calnexin (*CNX*, endoplasmic reticulum marker) or early endosome antigen 1 (*EEA1*, early endosome marker). No significantly difference in co-localization was observed. *D*, MDCK cells transfected with wild-type EGFP-tagged GlyT2 or Y705C were plated on cell culture filter inserts and grown to confluence. Samples were examined by laser scanning confocal microscopy. *Left panel*, en face views. *Right panel*, *x-z* cross-sections. The *x-z* cross-sections are derived from the indicated transept lines.

plasma membrane levels sufficiently to restore the wild-type levels of surface-active GlyT2. For this purpose, we treated COS7 cells expressing wild-type GlyT2 or the Y705C mutant with DTT for increasing periods of time up to 30 min and measured [^{3}H]glycine transport and surface biotinylation in parallel (Fig. 6, *A* and *B*). As shown above, glycine transport by the Y705C mutant was rapidly increased by DTT, reaching wild-type levels of activity in 3–4 min and continuing up to 10 min before reaching a plateau (Fig. 6*A*). A 10-min period has been shown to be sufficient for trafficking to the Golgi of polytopic proteins expressed in mammalian cells (29). We have measured comparable time courses of plasma membrane expression for GlyT2.[3] In fact, extended time periods in DTT increased the amount of surface mutant transporter with a slightly delayed time course. This indicates a fast activation of surface-inserted transporter (5 min) followed by a slower increase in the amount of plasma membrane protein (10–30 min; Fig. 6*B*, *left histogram*). A decrease in the levels of the immature protein was also observed (Fig. 6*B*, *right histogram*). By contrast, the quantity of wild-type GlyT2 present in the plasma membrane was slightly diminished by DTT, and the transport activity was only slightly

[3] E. Arribas-González, P. Alonso-Torres, C. Aragón, and B. López-Corcuera, manuscript in preparation.

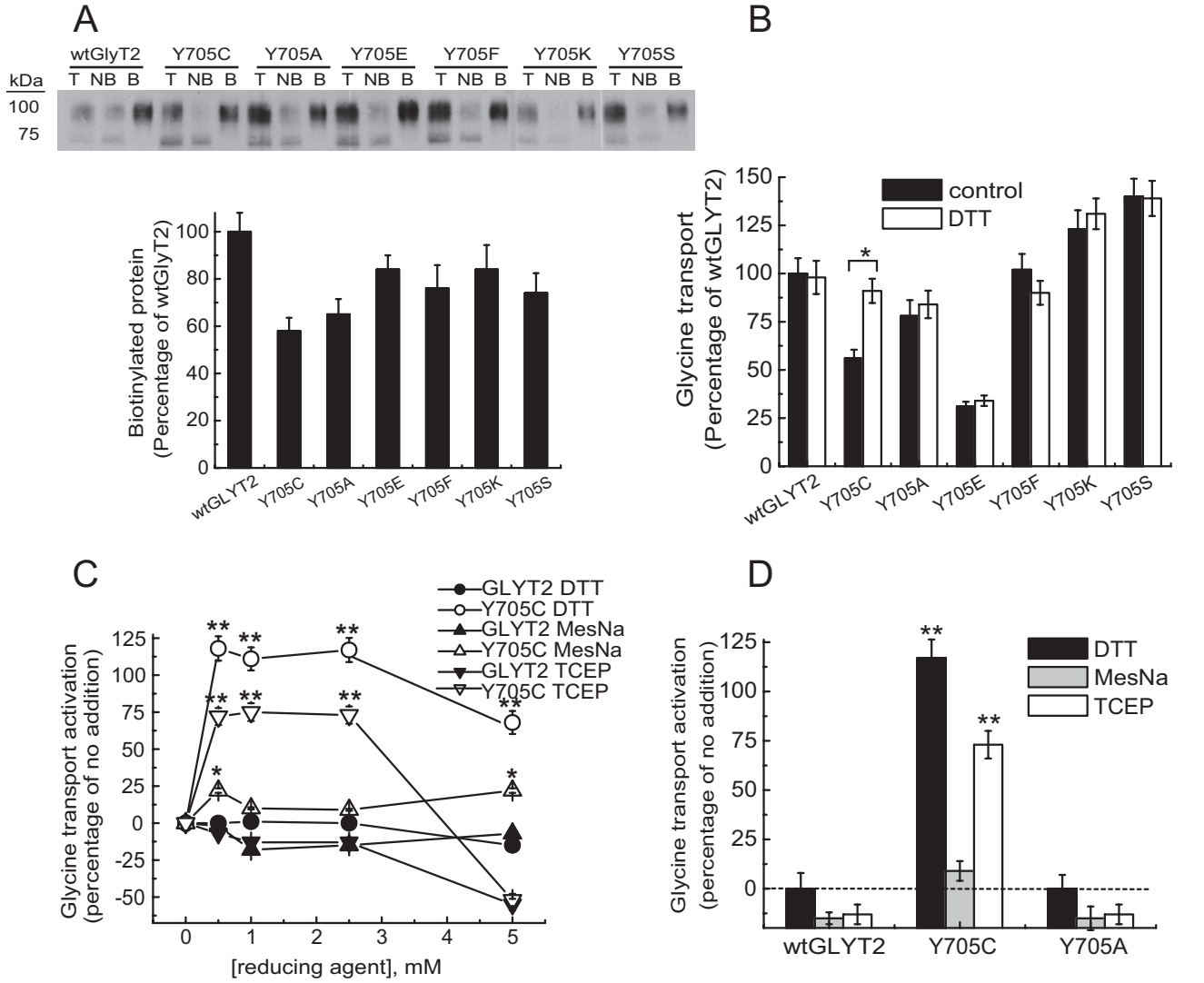

FIGURE 5. **Substitution analysis of Tyr-705 and effect of DTT on glycine transport.** Transiently transfected COS7 cells expressing wild-type GlyT2 or mutants with the indicated amino acids at position 705, were subjected to biotinylation as described in Fig. 4 to determine plasma membrane expression (*A*) or treated with vehicle or 12 mM DTT (*B*) or 2.5 mM DTT (*D*) or the specified concentrations of the indicated reducing agents (*C*) and then assayed for [^{3}H]glycine transport. In *B*, * indicates significantly different from wild-type GlyT2, $p < 0.05$ in Student's *t* test. In *C* and *D*, ** indicates $p < 0.01$, and * indicates $p < 0.05$ by analysis of variance. *Lanes T*, total proteins; *lanes NB*, nonbiotinylated proteins; *lanes B*, biotinylated proteins.

increased. To confirm that DTT can induce Y705C exocytosis, we treated MDCK cells expressing EGFP-tagged transporters with DTT and monitored co-localization with the plasma membrane marker E-cadherin (Fig. 6, *C* and *D*). As shown in Fig. 4*A*, the percentage of Y705C co-localization with the plasma membrane marker was ~65% compared with wild-type GlyT2, and the co-localization was increased by 40% by DTT (Fig. 6*D*).

Y705C Forms an Aberrant Disulfide Bond Interfering with the Cys-311–Cys-320 Pair—One possible explanation of the recovery of Y705C function with DTT could be that Cys-705 forms a disulfide bond with one of the 23 endogenous cysteines present in GlyT2 (Fig. 7*B*). Such a covalent bond could impair glycine transport and/or transporter trafficking. Cleavage of this bond by DTT could restore mutant membrane expression and transport activity. To test this possibility, we took advantage of the predicted external accessibility of Cys-705 and labeled the cells expressing the transporters with the nonpermeable SH-specific reagent MTSEA-biotin (Fig. 7, *A*, *E*, and *F*). This probe reacts with externally accessible free thiol groups in an aqueous environment. In control conditions, the fraction of SH-labeled Y705C mutant was higher than that of wild-type GlyT2 (~2 ± 0.5-fold; Fig. 7, *A* and *E*). Taking into account that the membrane expression of Y705C is ~65% of wild-type GlyT2 (Fig. 4), this means the cysteine specific label is ~3-fold higher in the Y705C mutant than in wild-type GlyT2. In fact, pretreatment with DTT, which increases mutant membrane expression to wild-type levels (Fig. 6), yielded ~3-fold higher labeling for Y705C compared with wild-type GlyT2 (Fig. 7, *A*, *E*, and *F*). This suggests that the Y705C mutation involves structural effects that increase cysteine availability. When the cells were pretreated with *N*-ethylmaleimide in the absence of DTT to prevent SH reagent reaction with the free cysteines, both transporters showed reduced labeling (Fig. 7*A*). Under this condition, the Y705C labeling was ~65% of that of wild-type GlyT2, reflecting lower membrane expression. Moreover, if *N*-ethyl-

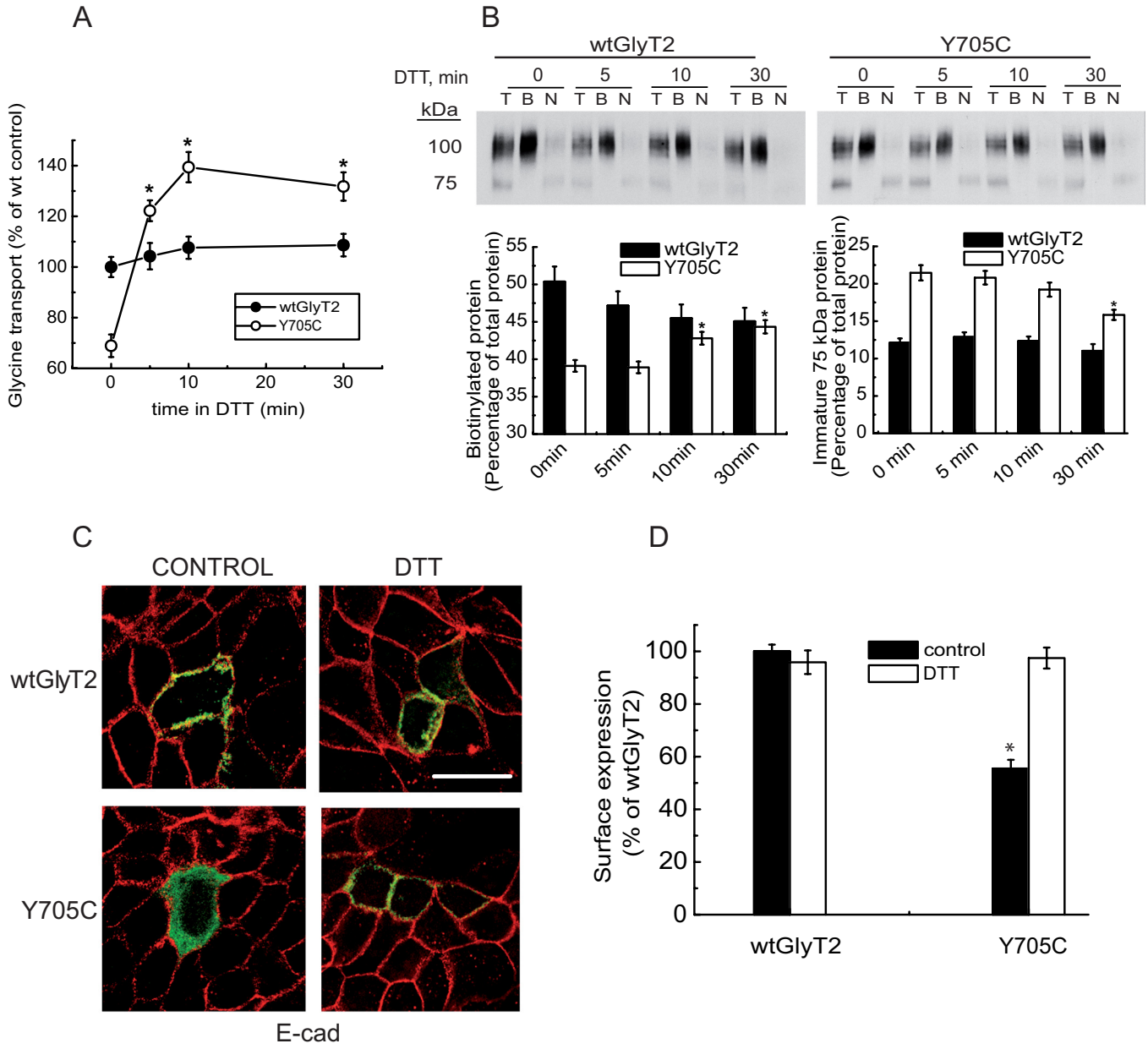

FIGURE 6. **Effect of DTT on Y705C plasma membrane expression.** COS7 cells expressing wild-type GlyT2 or Y705C were treated with 12 mM DTT at 22 °C for the indicated times and then assayed for [^{3}H]glycine transport for 10 min (*A*) or subjected to sulfo-NHS-SS-biotinylation as described under "Experimental Procedures" (*B*). *A*, transport data are expressed as percentages of wild-type GlyT2 transport activity, which was 2.8 ± 0.3 nmol of Gly/mg of protein/10 min. *, significantly different from no DTT, $p < 0.05$ in Student's *t* test. *B*, *upper panel*, Western blot for GlyT2 detection of a SDS-PAGE loaded with 8 μg of total (*lanes T*) and nonbiotinylated proteins (*lanes N*) and 24 μg of biotinylated proteins (*lanes B*). *Lower panel*, densitometric analysis. *, significantly different from no DTT, $p < 0.05$ in Student's *t* test. *C*, MDCK cells expressing wild-type EGFP-tagged GlyT2 or Y705C were treated for 30 min with 12 mM DTT, placed on ice to stop trafficking, and immunolabeled for the plasma membrane marker E-cadherin (*E-cad*). *D*, co-localization of transporter and marker was performed as described for Fig. 4. *, $p < 0.05$ values calculated using Student's *t* test by comparing wild-type GlyT2 with the Y705C mutant.

maleimide pretreatment was performed, and then DTT was added to release cysteines from disulfides, the DTT-induced increase in SH-specific label of the Y705C mutant was higher than that of wild-type GlyT2 (Fig. 7*A*). This result suggests the presence of an additional disulfide bond in the Y705C mutant. To identify the binding partner for Cys-705, we inspected the three-dimensional structure of GlyT2 and selected several cysteine residues based on location that might permit the formation of an intra- or intermolecular disulfide bond with Cys-705 (Fig. 7*B*). Selected cysteines were individually substituted to serine to form Cys → Ser mutants. Single substitutions were introduced into the Cys-705 background to generate double mutants (*CXS/Y705C*), which were tested for DTT activation of glycine transport (Fig. 7, *C* and *D*). Two of the mutants (C311S/Y705C and C320S/Y705C) were activated to a smaller extent than the other mutants (Fig. 7*D*). This result supports a potential interaction between a cysteine at position 705 and cysteines at positions 311 and 320. Accordingly, C311S/Y705C or C320S/Y705C double mutants display a significantly reduced MTSEA-biotin labeling compared with the Y705C mutant, indicating that Cys-705 can interact with either Cys-311 or Cys-320 (Fig. 7, *E* and *F*). Cysteines 311 and 320 are located in the second

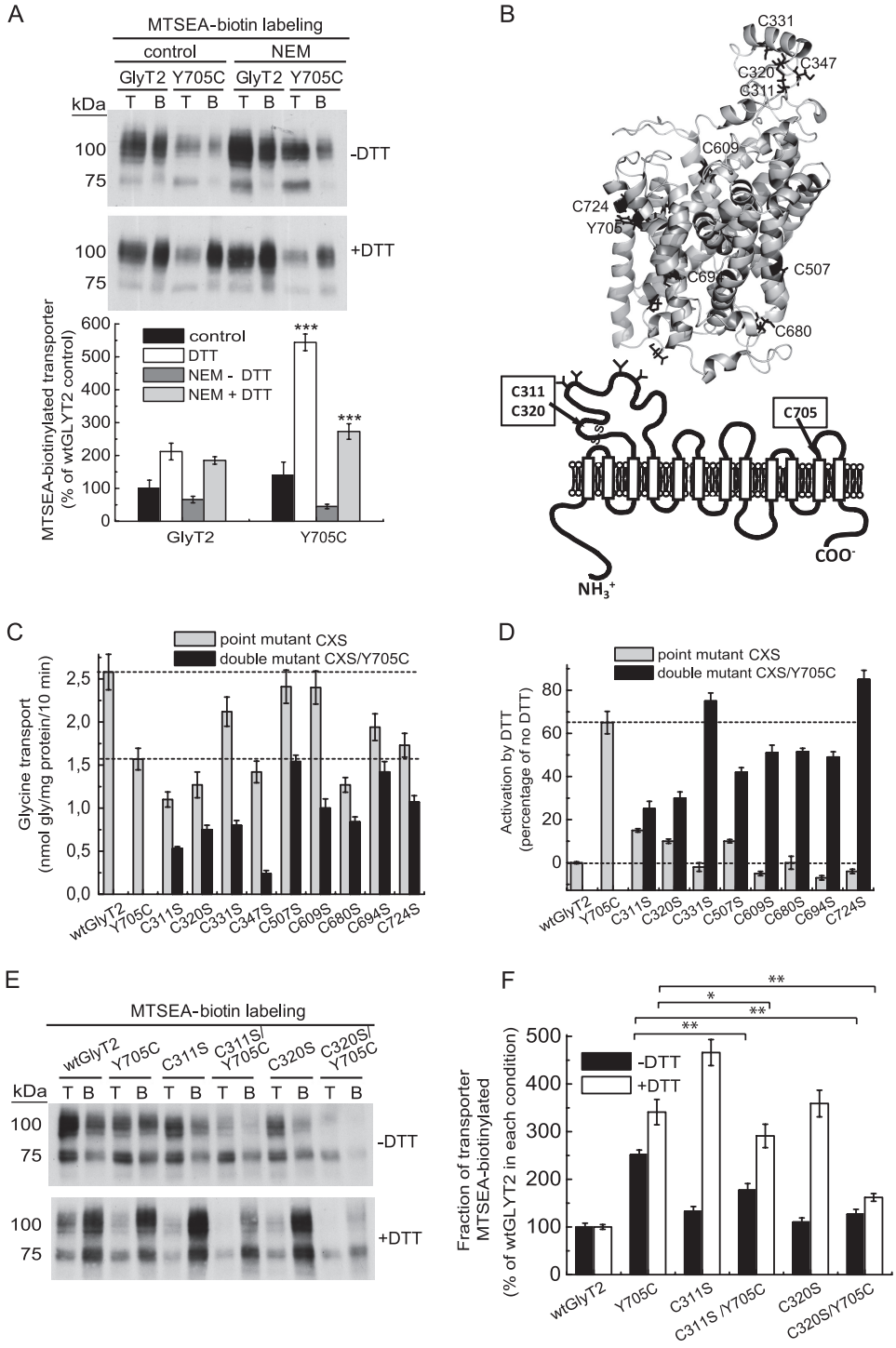

FIGURE 7. **MTSEA-biotin labeling and transport activity of Y705C and GlyT2 cysteine mutants.** *A*, COS7 cells expressing wild-type GlyT2 or Y705C were treated with vehicle or 50 mM *N*-ethylmaleimide (*NEM*) for 10 min, washed, and treated with HBS or 12 mM DTT in HBS for 30 min, washed, and subjected to MTSEA-biotinylation as described under "Experimental Procedures." *Upper panel*, Western blot for GlyT2 detection of a SDS-PAGE loaded with 10 μg of total (*lanes T*) and 100 μg of biotinylated proteins (*lanes B*). *Lower panel*, densitometric analysis of the percentage of total transporter (*B* as a % of *T*) that was MTSEA-biotin-labeled in each condition as percentage of control wild-type GlyT2. ***, Significantly different from wild-type GlyT2, $p < 0.001$ in Student's *t* test. *B*, *upper panel*, molecular model of GlyT2 showing the localization of Tyr-705 and some of the endogenous cysteines (*black*). *Lower panel*, location of the Cys-311–Cys-320 pair in the second external loop as compared with Cys-705 on schematic GlyT2 secondary structure. *C* and *D*, effect of DTT on glycine transport by cysteine to serine mutants in the background of wild-type GlyT2 or the Y705C mutant. COS7 cells expressing wild-type GlyT2, Y705C, cysteine to serine mutants (*CXS*), or Y705C/cysteine to serine double mutants (*CXS/Y705C*) for 48 h were assayed for [^{3}H]glycine transport for 10 min after being treated with vehicle (*C*) or with 12 mM DTT at 22 °C for 5 min (*D*). *E*, COS7 cells expressing the indicated transporters were treated with vehicle (−DTT) or DTT (+DTT) for 30 min, washed, and MTSEA-biotin-labeled; streptavidin-agarose bound proteins were run in nonreducing (−*DTT*) or reducing (+*DTT*) SDS-PAGE and subjected to Western blotting as above. *F*, densitometric analysis of the percentage of total transporter that was MTSEA-biotin-labeled in each condition. For clarity, this was expressed as percentage of the respective wild-type GlyT2 in each condition. Significantly different from the Y705C single mutant: *, $p < 0.05$; **, $p < 0.01$ in Student's *t* test.

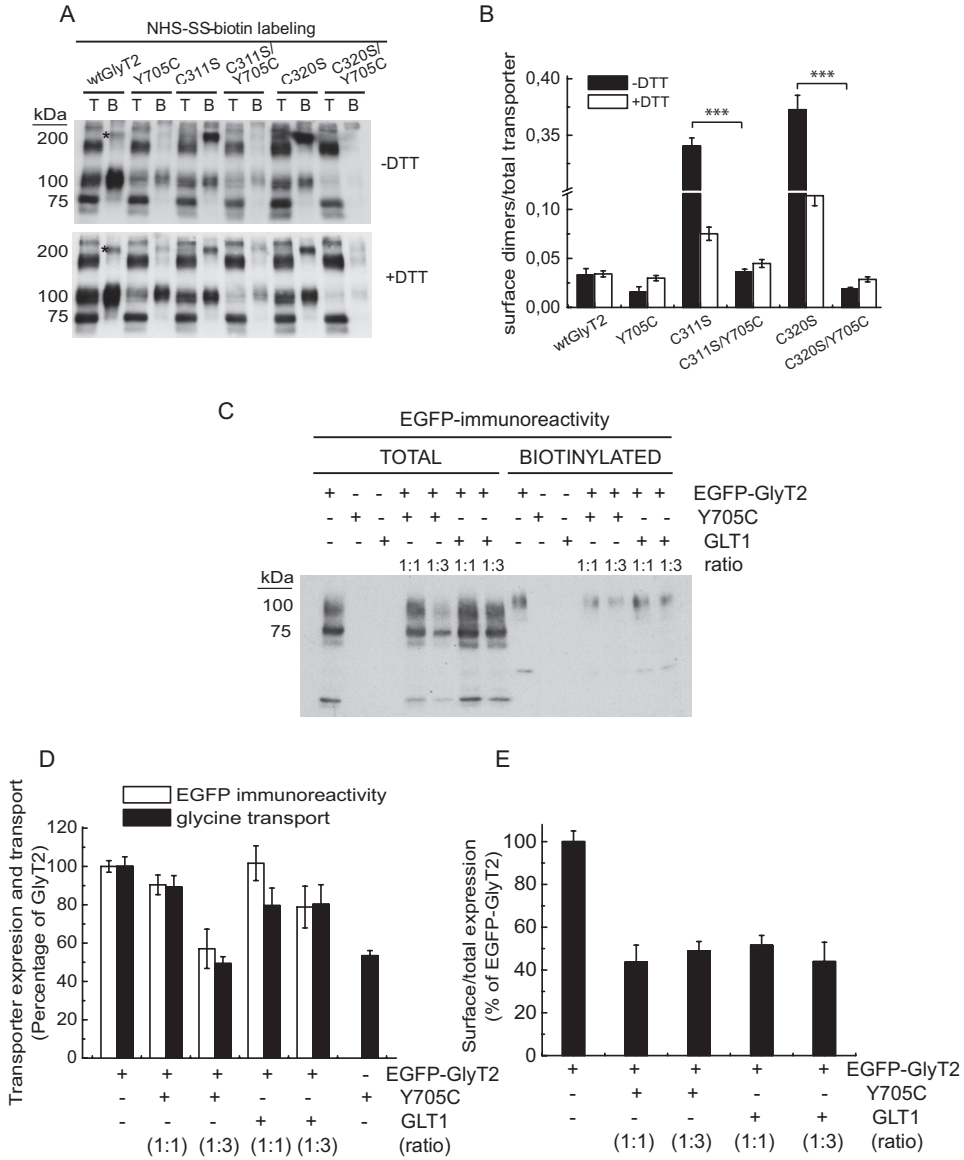

FIGURE 8. **Surface labeling and co-expression of Y705C and GlyT2 cysteine mutants.** *A*, COS7 cells expressing the indicated transporters were treated with vehicle (−*DTT*) or DTT (+*DTT*) for 30 min, washed, and subjected to NHS-SS-biotinylation as in Fig. 4*B*. *Lanes T*, total proteins; *lanes B*, biotinylated proteins. *B*, densitometric analysis of three blots as in *A* showing the immunoreactivity of 200-kDa dimers (*band* marked with *asterisk* in *A*) normalized by the total transporter immunoreactivity. ***, significantly different from the respective single mutant, $p < 0.01$ in Student's *t* test. *C*, effect of wild-type GlyT2 and Y705C on transporter expression. COS7 cells expressing wild-type GlyT2 or Y705C tagged with EGFP as described in Ref. 24 at the indicated ratios (increasing mutant cDNA) were assayed for [^{3}H]glycine transport and in parallel subjected to NHS-SS-biotinylation as described under "Experimental Procedures" except anti-EGFP antibody was used for the Western blots. *D*, effect of the expression of Y705C on EGFP-GlyT2 expression (densitometric analysis of blots as in *C*) and transport activity. *E*, effect of the expression of Y705C on EGFP-GlyT2 surface expression.

external loop (EL2) of GlyT2 (Fig. 7*B*). This region cannot currently be accurately modeled because of significant divergence in sequence and length compared with $LeuT_{Aa}$ (18, 21). However, equivalent conserved cysteines have been shown to form a disulfide bond in other members of the SLC6 family (30, 31). Unexpectedly, although C311S and C320S mutants should both have a single unpaired extracellular cysteine like Y705C, they have much lower cysteine labeling in the absence of DTT. In addition, they display very high MTSEA-biotin label after DTT treatment (Fig. 7, *E* and *F*). This unexpected result made us consider the possibility that the unpaired cysteine from the Cys-311–Cys-320 disulfide might form a disulfide bond with another monomer, creating disulfide-linked dimers. Fig. 8*A* shows that C311S and C320S mutants form disulfide-mediated dimers on the cell surface (band indicated by an *asterisk*), which are cleaved to monomers in the double C311S/Y705C or C320S/Y705C mutants. This reinforces the evidence that Cys-705 interacts with Cys-311 and Cys-320 (Fig. 8*B*).

A further relevant question is whether the trafficking defect of Y705C affects the expression of wild-type GlyT2. To answer this, we co-expressed wild-type and mutant GlyT2 differentially tagged with EGFP (Fig. 8*C*). The Y705C mutant reduces total wild-type GlyT2 expression by 10–20% when expressed at 1:1 ratio. This is comparable with the effect of a nonrelevant protein, the glutamate transporter GLT1 (Fig. 8*D*). At a higher GlyT2-Y705C ratio (1:3), a slight reduction of GlyT2 expression by the Y705C mutant was observed, although this effect was not due to a reduced delivery to the plasma membrane (Fig. 8*E*). Moreover, wild-type GlyT2 co-

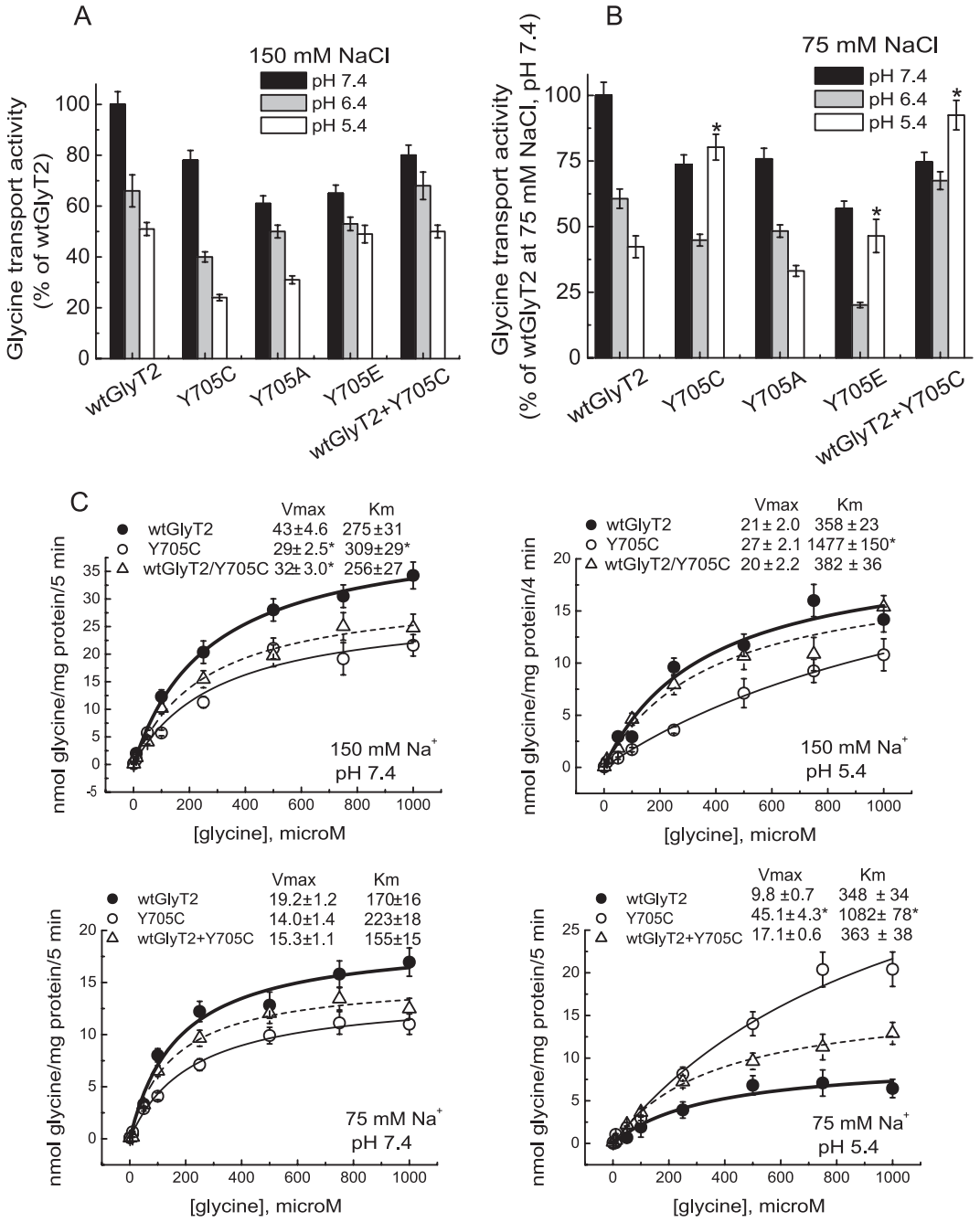

FIGURE 9. **Effect of pH on glycine transport by wild-type GlyT2 and the Tyr-705 mutant.** Transiently transfected COS7 cells expressing wild-type GlyT2 or mutants with the indicated amino acid substitutions at position 705 were assayed for [^{3}H]glycine transport for 5 min in HBS containing 150 (*A* and *C*) or 75 (*B* and *C*) mM NaCl at 10 μM or the indicated final glycine concentration and pH. Control GlyT2 transport values at pH 7.4 were 1.4 $\pm$ 0.2 and 0.73 $\pm$ 0.1 nmol of Gly/mg of protein/5 min at 150 and 75 mM NaCl, respectively. Mean pH change was significantly different from wild-type GlyT2. *, $p < 0.05$ by analysis of variance with Dunnett's post hoc test. *C*, kinetics of glycine transport at low pH. COS7 cells expressing wild-type GlyT2, the Y705C mutant, or the indicated combination of the respective cDNAs were assayed for [^{3}H]glycine transport at pH 7.4 or 5.4 for 5 min in HBS containing 150 or 75 mM NaCl and glycine concentrations increasing from 0.5 μM to 1 mM. Experimental data were fitted to hyperbolae. The kinetic parameters are indicated on the graphs. Mean pH change significantly different from wild-type GlyT2. *, $p < 0.05$ in Student's *t* test.

expressed with Y705C reduces the expression of the mutant by ~10–20% (data not shown). These results indicate that the traffic defect of the Y705C mutant is not dominant when it is co-expressed at the same dose as wild-type GlyT2.

H^+ Dependence of Glycine Transport Is Inverted in the Y705C Mutant—According to the above data, DTT is likely to disrupt an aberrant disulfide bond in the Y705C mutant. This facilitates exocytosis and induces the emergence of the mutant transporter on the cell surface. In addition, the Y705C substitution predicts the introduction of a local negative charge on the surface of the transporter because of the more acidic nature of the cysteine side chain (pK_a of 8.3 *versus* 10.3 for tyrosine). Because the protonation state of protein ionizable groups is dependent on pH, we tested the pH dependence of Tyr-705 mutants containing titratable side chains (Fig. 9). In agreement with published data on GABA transporters (32, 33), wild-type GlyT2 is

inhibited at low pH, showing ~50–60% transport activity at pH 5.4. The inhibition was even higher when assayed in low external sodium (Fig. 9, *A* and *B*). This is in agreement with the proposed competition of the two cations in the external transporter vestibule (32, 33). When the assay was performed at the physiological NaCl concentration (150 mM), the wild-type response to low pH was also observed for the Y705C, Y705E, and Y705A mutants (Fig. 9*A*). However, lowering the external pH in the presence of low NaCl concentrations (75 mM) produced a differential response in the Y705C and Y705E mutants. They became activated at pH 5.4 instead of inhibited, indicating an altered proton dependence of transport in these Tyr-705 substitutions (Fig. 9*B*). Furthermore, the pH dependence of wild-type GlyT2 co-transfected at a 1:1 cDNA ratio with the Y705C mutant resembled that of the mutant rather than wild-type GlyT2. This suggests a dominant phenotype for Y705C (Fig. 9, *A* and *B*). Therefore, we characterized the transport kinetics at acidic pH (Fig. 9*C*). The Y705C mutant had increased V_{max} at pH 5.4 when expressed alone and in co-expression with wild-type, especially at low sodium. This is in contrast to wild-type GlyT2 that showed a ~50% reduction in V_{max} value at acidic *versus* neutral pH. In addition, a general increase in K_m at low pH was observed for all the transporters. This was more pronounced for Y705C and the co-expression, especially at low sodium (~2-, 5-, and 2.5-fold for wild-type GlyT2, Y705C, and Y705C+wild-type GlyT2, respectively). Taken together, these data indicate that the Y705C mutation in GlyT2 induces an altered response to proton modulation of glycine transport.

Y705C Mutant Is Partially Resistant to Zn^{2+} Inhibition of Glycine Transport—Protons and metal transition dications are competitive inhibitors of several crucial mediators of glycinergic neurotransmission, such as the glycine receptor (34–36) and the glycine transporter GlyT1 (37, 38). Because H^+ and Zn^{2+} frequently bind to overlapping intersubunit sites (39–41), and the binding of transition dications can induce cysteine deprotonation (42), we tested the effect of Y705C substitution on the sensitivity of GlyT2 to Zn^{2+}. Although GlyT2 is not very sensitive to this cation (38), we observed a low but significant inhibition of GlyT2 transport by Zn^{2+} (Fig. 10). As expected, we found that Zn^{2+} sensitivity of wild-type transport was pH-dependent, being higher at pH 7.4 than 5.4, in agreement with the competitive nature of H^+ and Zn^{2+} inhibition (35, 38, 39). By contrast, the inhibition by Zn^{2+} of the Y705C mutant was much less sensitive to the presence of protons and slightly more pronounced at acidic pH. As expected from the proton response shown above, the co-expression of wild-type GlyT2 and the Y705C mutant also resulted in Y705C behavior, confirming a dominant phenotype (Fig. 10*A*). Fig. 10*B* shows that the IC_{50} for Zn^{2+} inhibition of wild-type GlyT2 was significantly increased at acidic pH from 63 ± 10 at pH 7.4 to 466 ± 42 μM at pH 5.4. By contrast, the Y705C mutant had IC_{50} values of 100 ± 15 and 189 ± 19 μM at these same pH values. The co-expressed wild-type GlyT2 and Y705C mutant displayed IC_{50} values of 99 ± 10 and 198 ± 22 μM, which are close to those of Y705C mutants. Further kinetic analysis of glycine transport in the presence of Zn^{2+} showed a significantly lower decrease in the V_{max} of transport by the Y705C-containing transporters than for wild-type GlyT2. In addition, a higher increase in K_m was observed. These data confirm the reduced sensitivity of Y705C-containing glycine transporters to Zn^{2+} inhibition (Fig. 10*C*).

DISCUSSION

We have identified a novel missense mutation in *SLC6A5*, encoding GlyT2, present in eight individuals from three families in two cohorts of hyperekplexia patients from Spain and the United Kingdom. The mutation results in a tyrosine to cysteine substitution at residue 705 (Y705C) in transmembrane domain 11 (TM11). This change was found in the heterozygous state in all positive cases suggesting a dominant mode of inheritance. This contrasts with the majority of the previously characterized GlyT2 mutations that were inherited in a recessive or compound heterozygous state (11). Y705C-harboring patients show significant variability in clinical presentation. As well as classical hyperekplexia symptoms, certain individuals exhibited abnormal respiration, facial dysmorphism, delayed motor development, or intellectual disability. This may be due to a complex phenotype caused by the mutation or to the presence of additional unknown mutations or modifiers. However, no other potential disease-causing mutations were detected in *SLC6A5*. Study of the biochemical properties of the mutant transporter in cultured cells revealed that the introduced cysteine affects several aspects of transporter biochemistry. These include impaired transporter protein maturation through the secretory pathway and an alteration of H^+ and Zn^{2+} dependence of glycine transport. The latter feature constitutes a dominant effect, because it is observed when the mutant is expressed alone and also when mutant and wild-type transporters are co-expressed.

The Y705C substitution introduces a free thiol in the place of a hydroxyl-containing side chain. Thiol labeling with impermeant cysteine MTS reagents confirmed that Cys-705 is accessible from the exterior of the plasma membrane, as predicted by molecular modeling. Therefore, the Y705C mutant exposes the introduced cysteine to the lumen of the secretory pathway cisternae during trafficking. This seems to be detrimental for transporter biogenesis, because Y705C has reduced expression at the plasma membrane, together with a higher proportion of immature precursor compared with wild-type GlyT2. This is in agreement with recent reports indicating that polymorphisms containing an uneven number of cysteine residues in extracellular loops impair the expression of G-protein-coupled receptors and other plasma membrane proteins. This feature has frequently been associated with disease states (29, 43–45). Restoration of Y705C membrane expression to wild-type levels with the permeable thiol reagent DTT and experiments using SH-specific and surface labeling of cells expressing the transporters suggest that Cys-705 is involved in aberrant disulfide bond formation. Cys-705 binding partners are either of two EL2 cysteines that are likely to form a disulfide bond in wild-type GlyT2 (C311-C320 pair) (30, 31). This interference is probably conformation-dependent, because EL2 may approach TM11 during the inward-facing conformation (46). Disruption of this aberrant bond with reducing agents may facilitate plasma membrane arrival and/or the conformational movements needed for transport in the surface-resident transporter. How-

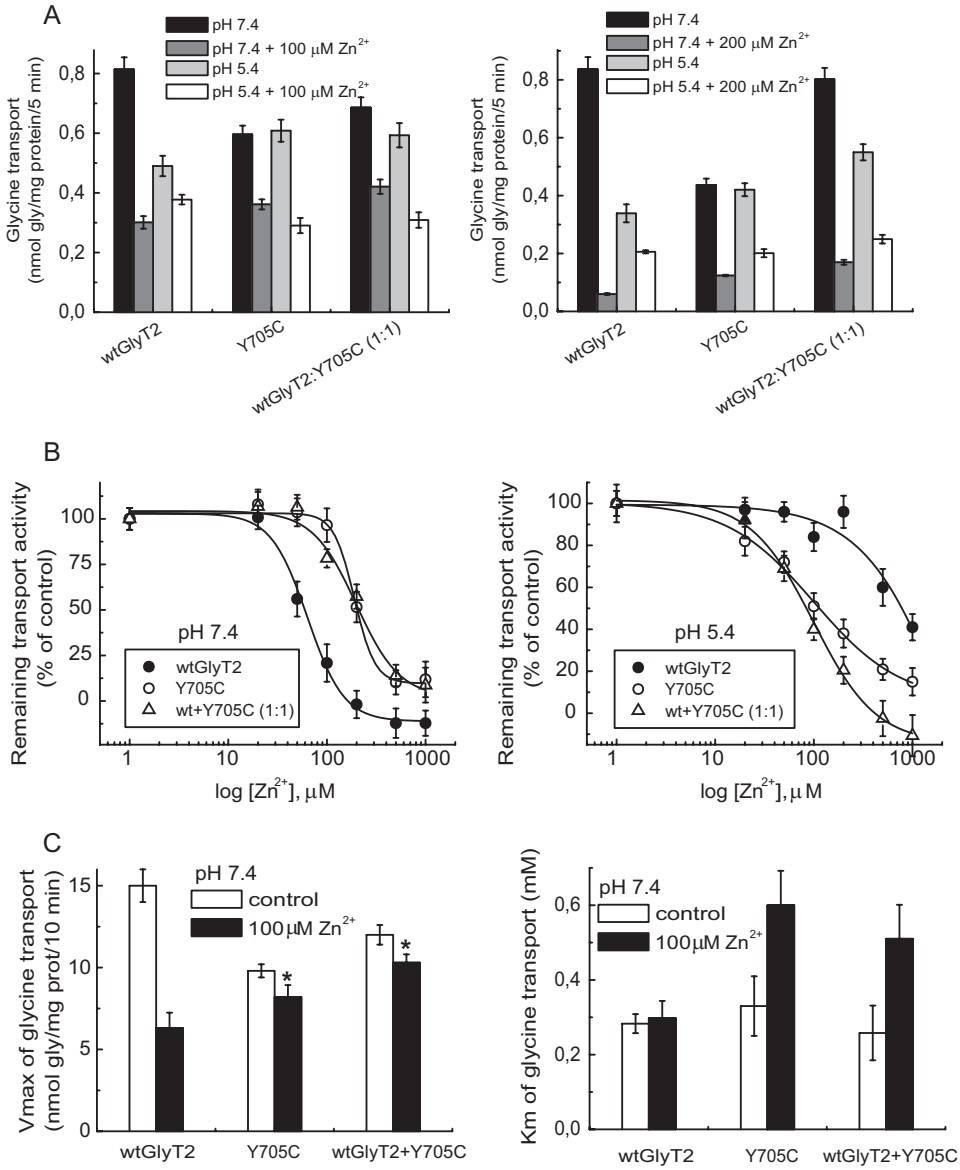

FIGURE 10. **Effect of Zn^{2+} on glycine transport by wild-type GlyT2 and the Y705C mutant.** Transiently transfected COS7 cells expressing wild-type GlyT2, the Y705C mutant, or the indicated combinations of the respective cDNAs were assayed for [^{3}H]glycine transport for 5 min in HBS containing 75 mM NaCl at the indicated pH and 10 μM final glycine concentration (*A* and *B*) or increasing glycine concentrations (*C*) in the presence of the indicated ZnCl concentrations (*A–C*). NaCl was isotonically substituted by choline chloride. *B*, dose-response data were fit to logistic curves. *C*, transport data were fitted to hyperbolae, and kinetic parameters were obtained from the best fit. Mean change significantly different from wild-type GlyT2. *, $p < 0.05$ in Student's *t* test.

ever, it is not clear whether Y705C expression is lower because a proper disulfide bridge cannot be formed or because the aberrant disulfide bond distorts the protein structure, because both conditions are present in Y705C. The single C311S and C320S mutants show approximately half the membrane expression of wild-type GlyT2, suggesting that the lack of the endogenous disulfide bond is detrimental for surface expression. However, the unusual behavior of these mutants prevents us from drawing clear conclusions. The fact that Y705C and wild-type GlyT2 are differentially sensitive to low concentrations of reducing agents but are inhibited by higher concentrations (Fig. 5*C* and data not shown) suggests that the aberrant disulfide bond involving Cys-705 is more sensitive to cleavage than the Cys-311–Cys-320 disulfide bond. The recovery of the expression in the Y705C mutant might be due to the cleavage of aberrant disulfide bonds without affecting the Cys-311–Cys-320 pairing. It is also possible that GlyT2 requires disulfide-mediated dimerization for plasma membrane expression as has been suggested for other SLC6 transporters (31) and that this process is disrupted by the Y705C mutation. Because GlyT2 multimerization has been proposed to be required for plasma membrane localization (47), this is an issue that will require further study.

The Y705C substitution is also predicted to introduce a local negative charge at the transporter surface. The endogenous Tyr-705 residue with a typical pK_a value of ~10.3 would be mostly protonated at physiological pH. By contrast, the side chain of Cys-705 would, in theory, be also protonated, but the more acidic pK_a value (close to 8.3) makes the probability of ionization higher than for the tyrosine side chain. In addition, a high dielectric medium favors cysteine deprotonation, whereas

a low dielectric medium favors the protonated state (42). Because Cys-705 is extracellular, it is therefore likely to be in a high dielectric environment. Deprotonation is also favored by the presence of transition metal dications, which may perform a metal-assisted deprotonation of cysteine side chains, especially if bound to polarizable ligands (42). Other factors such as the possible hydrogen-bonding network including the cysteine may affect the pK_a (48). All of these factors may drive Cys-705 to be deprotonated at physiological pH. By contrast, acidic pH may displace the equilibrium toward the protonated form. GlyT2 transport activity seems to be sensitive to the protonation state of Cys-705, and protonation may activate the mutant transporter. Therefore, although glycine transport by wild-type GlyT2 is inhibited at low pH, the Y705C mutant is resistant to this inhibition.

Functional analysis of the Y705C mutant has revealed the existence of an unexpected fine-tuning mechanism of glycine transport by external H^+, with Tyr-705 playing a central role. Interestingly, the GlyR is also inhibited by protons and the proton-binding site also involves a hydroxyl-containing residue (Thr-112), which when substituted by a tyrosine (but not by a neutral amino acid) preserves the H^+ sensitivity of the receptor (49). Both Tyr-705 in GlyT2 and Thr-112 in GlyRs are highly conserved. A threonine is found at the equivalent position in all pH-sensitive GlyR, $GABA_A$, and $GABA_C$ receptors. Equally, a Tyr-705 equivalent is found in many SLC6 family members, suggesting that this tyrosine might have a general role in pH sensitivity of Na^+-and Cl^--dependent neurotransmitter transporters. The location of Tyr-705 in an extracellular accessible region of the transporter would fulfill one of the prerequisites for H^+-binding sites, which are usually located outside the membrane electric field (49, 50). Proton and transition dication binding sites are usually overlapping in pH- and Zn^{2+}-sensitive proteins (34–36, 38). In the GlyR, Thr-112 also forms part of the group of crucial residues involved in regulation by Zn^{2+} (35). In several plasma membrane proteins present in inhibitory synapses, H^+/Zn^{2+}-binding sites are contributed by several adjacent subunits (35, 49, 51, 52). This structural requirement might also hold true for GlyT2 and would sustain the dominant nature of the aberrant pH sensitivity and Zn^{2+} dependence of the Y705C mutant co-expressed with wild-type GlyT2.

In summary, we have identified a novel missense mutation in GlyT2 associated with hyperekplexia and described altered biochemical properties of the mutant transporter. The Y705C mutation affects several aspects of transporter biochemistry including impaired transporter protein maturation through the secretory pathway and an alteration of H^+ and Zn^{2+} dependence of glycine transport. Any of these features may contribute to the etiology of the disease. In addition to effects in pathophysiological conditions such as inflammation and ischemia, transient changes in extracellular pH occur under physiological conditions. For example, in synaptic transmission, the acidic contents of transmitter vesicles cause an extracellular acid shift within the synaptic cleft (53, 54) and may reduce the local Na^+ concentration. Different sources of protons have been suggested in the synapse: acidic contents after vesicle fusion, incorporation of the vesicular ATPase to the plasma membrane, or extrasynaptic sources such as H^+ ion exchangers and voltage-gated H^+ conductances (51). These pH changes are especially relevant during repetitive electrical stimulation that may produce acid shifts of ~30 s in duration (53). Acidification reduces the duration of glycinergic synaptic currents and accelerates desensitization of the receptor significantly affecting the kinetics of glycinergic neurotransmission (54). Increased external pH potentiated, whereas decrease inhibited both the amplitude and frequency of glycinergic miniature inhibitory postsynaptic potential currents, suggesting the involvement of both presynaptic and postsynaptic mechanisms (54). In addition, Zn^{2+} is highly enriched in synaptic vesicles, from which it can be co-released with glutamate in an activity-dependent manner (36). Zn^{2+} modulates both current responses mediated by excitatory and inhibitory neurotransmitter receptors and the efficacy of transporter-driven neurotransmitter reuptake (55). We hypothesize that Y705C mutant may alter the kinetics of glycinergic inhibition by taking up glycine when the transporter is supposed to be inhibited by synaptic H^+ or Zn^{2+}. This may disrupt the coordination of neurotransmitter release and subsequent reuptake, leading to a damaging effect, mainly during repetitive firing. In addition, the mutant transport activity, which is resistant to two "natural" synaptic inhibitors, may prevent or dampen the interaction of glycine with GlyRs by simple competition. Finally, defective trafficking of the mutant may reduce the uptake of glycine at neutral pH, thus reducing the availability of transmitter in the terminal for synaptic vesicle loading. Future work performed in neuronal preparations will reveal to what extent glycinergic neurotransmission is impaired by the Y705C mutation.

Acknowledgments—We acknowledge the expert technical assistance of the confocal microscopy facility at the Centro de Biología Molecular "Severo Ochoa" (Madrid, Spain). Carlos Ernesto Fernández García is also acknowledged.

REFERENCES

1. Aragón, C., and López-Corcuera, B. (2003) Structure, function and regulation of glycine neurotransporters. *Eur. J. Pharmacol.* **479,** 249–262
2. Gomeza, J., Hülsmann, S., Ohno, K., Eulenburg, V., Szöke, K., Richter, D., and Betz, H. (2003) Inactivation of the glycine transporter 1 gene discloses vital role of glial glycine uptake in glycinergic inhibition. *Neuron* **40,** 785–796
3. Aragón, C., and López-Corcuera, B. (2005) Glycine transporters. Crucial roles of pharmacological interest revealed by gene deletion. *Trends Pharmacol. Sci.* **26,** 283–286
4. Gomeza, J., Ohno, K., Hülsmann, S., Armsen, W., Eulenburg, V., Richter, D. W., Laube, B., and Betz, H. (2003) Deletion of the mouse glycine transporter 2 results in a hyperekplexia phenotype and postnatal lethality. *Neuron* **40,** 797–806
5. Gomeza, J., Ohno, K., and Betz, H. (2003) Glycine transporter isoforms in the mammalian central nervous system. Structures, functions and therapeutic promises. *Curr. Opin. Drug Discov. Devel.* **6,** 675–682
6. Harvey, R. J., Topf, M., Harvey, K., and Rees, M. I. (2008) The genetics of hyperekplexia. More than startle!. *Trends Genet.* **24,** 439–447
7. Andermann, F., Keene, D. L., Andermann, E., and Quesney, L. F. (1980) Startle disease or hyperekplexia. Further delineation of the syndrome. *Brain* **103,** 985–997
8. Rees, M. I., Harvey, K., Pearce, B. R., Chung, S. K., Duguid, I. C., Thomas, P., Beatty, S., Graham, G. E., Armstrong, L., Shiang, R., Abbott, K. J., Zuberi, S. M., Stephenson, J. B., Owen, M. J., Tijssen, M. A., van den Maagdenberg, A. M., Smart, T. G., Supplisson, S., and Harvey, R. J. (2006) Mutations in the gene encoding GlyT2 (*SLC6A5*) define a presynaptic

component of human startle disease. *Nat. Genet.* **38,** 801–806
9. Rees, M. I., Harvey, K., Ward, H., White, J. H., Evans, L., Duguid, I. C., Hsu, C. C., Coleman, S. L., Miller, J., Baer, K., Waldvogel, H. J., Gibbon, F., Smart, T. G., Owen, M. J., Harvey, R. J., and Snell, R. G. (2003) Isoform heterogeneity of the human gephyrin gene (*GPHN*), binding domains to the glycine receptor, and mutation analysis in hyperekplexia. *J. Biol. Chem.* **278,** 24688–24696
10. Harvey, R. J., Depner, U. B., Wässle, H., Ahmadi, S., Heindl, C., Reinold, H., Smart, T. G., Harvey, K., Schütz, B., Abo-Salem, O. M., Zimmer, A., Poisbeau, P., Welzl, H., Wolfer, D. P., Betz, H., Zeilhofer, H. U., and Müller, U. (2004) GlyR α3. An essential target for spinal PGE_2-mediated inflammatory pain sensitization. *Science* **304,** 884–887
11. Chung, S. K., Vanbellinghen, J. F., Mullins, J. G., Robinson, A., Hantke, J., Hammond, C. L., Gilbert, D. F., Freilinger, M., Ryan, M., Kruer, M. C., Masri, A., Gurses, C., Ferrie, C., Harvey, K., Shiang, R., Christodoulou, J., Andermann, F., Andermann, E., Thomas, R. H., Harvey, R. J., Lynch, J. W., and Rees, M. I. (2010) Pathophysiological mechanisms of dominant and recessive *GLRA1* mutations in hyperekplexia. *J. Neurosci.* **30,** 9612–9620
12. Eulenburg, V., Becker, K., Gomeza, J., Schmitt, B., Becker, C. M., and Betz, H. (2006) Mutations within the human GLYT2 (*SLC6A5*) gene associated with hyperekplexia. *Biochem. Biophys. Res. Commun.* **348,** 400–405
13. Yamashita, A., Singh, S. K., Kawate, T., Jin, Y., and Gouaux, E. (2005) Crystal structure of a bacterial homologue of Na^+/Cl^--dependent neurotransmitter transporters. *Nature* **437,** 215–223
14. Haliassos, A., Chomel, J. C., Tesson, L., Baudis, M., Kruh, J., Kaplan, J. C., and Kitzis, A. (1989) Modification of enzymatically amplified DNA for the detection of point mutations. *Nucleic Acids Res.* **17,** 3606
15. Larkin, M. A., Blackshields, G., Brown, N. P., Chenna, R., McGettigan, P. A., McWilliam, H., Valentin, F., Wallace, I. M., Wilm, A., Lopez, R., Thompson, J. D., Gibson, T. J., and Higgins, D. G. (2007) Clustal W and Clustal X version 2.0. *Bioinformatics* **23,** 2947–2948
16. Ramensky, V., Bork, P., and Sunyaev, S. (2002) Human non-synonymous SNPs. Server and survey. *Nucleic Acids Res.* **30,** 3894–3900
17. Sali, A., and Blundell, T. L. (1993) Comparative protein modelling by satisfaction of spatial restraints. *J. Mol. Biol.* **234,** 779–815
18. Pérez-Siles, G., Morreale, A., Leo-Macías, A., Pita, G., Ortíz, A. R., Aragón, C., and López-Corcuera, B. (2011) Molecular basis of the differential interaction with lithium of glycine transporters GLYT1 and GLYT2. *J. Neurochem.* **118,** 195–204
19. Fornés, A., Núñez, E., Aragón, C., and López-Corcuera, B. (2004) The second intracellular loop of the glycine transporter 2 contains crucial residues for glycine transport and phorbol ester-induced regulation. *J. Biol. Chem.* **279,** 22934–22943
20. Pérez-Siles, G., Núñez, E., Morreale, A., Jiménez, E., Leo-Macías, A., Pita, G., Cherubino, F., Sangaletti, R., Bossi, E., Ortíz, A. R., Aragón, C., and López-Corcuera, B. (2012) An aspartate residue in the external vestibule of GLYT2 (glycine transporter 2) controls cation access and transport coupling. *Biochem. J.* **442,** 323–334
21. Jiménez, E., Zafra, F., Pérez-Sen, R., Delicado, E. G., Miras-Portugal, M. T., Aragón, C., and López-Corcuera, B. (2011) P2Y purinergic regulation of the glycine neurotransmitter transporters. *J. Biol. Chem.* **286,** 10712–10724
22. Núñez, E., Pérez-Siles, G., Rodenstein, L., Alonso-Torres, P., Zafra, F., Jiménez, E., Aragón, C., and López-Corcuera, B. (2009) Subcellular localization of the neuronal glycine transporter GLYT2 in brainstem. *Traffic* **10,** 829–843
23. Fornés, A., Núñez, E., Alonso-Torres, P., Aragón, C., and López-Corcuera, B. (2008) Trafficking properties and activity regulation of the neuronal glycine transporter GLYT2 by protein kinase C. *Biochem. J.* **412,** 495–506
24. de Juan-Sanz, J., Zafra, F., López-Corcuera, B., and Aragón, C. (2011) Endocytosis of the neuronal glycine transporter GLYT2. Role of membrane rafts and protein kinase C-dependent ubiquitination. *Traffic* **12,** 1850–1867
25. López-Corcuera, B., Martínez-Maza, R., Núñez, E., Roux, M., Supplisson, S., and Aragón, C. (1998) Differential properties of two stably expressed brain-specific glycine transporters. *J. Neurochem.* **71,** 2211–2219
26. Martínez-Maza, R., Poyatos, I., López-Corcuera, B., Núñez, E., Giménez, C., Zafra, F., and Aragón, C. (2001) The role of *N*-glycosylation in transport to the plasma membrane and sorting of the neuronal glycine transporter GLYT2. *J. Biol. Chem.* **276,** 2168–2173
27. Dunn, S. M., Conti-Tronconi, B. M., and Raftery, M. A. (1986) Acetylcholine receptor dimers are stabilized by extracellular disulfide bonding. *Biochem. Biophys. Res. Commun.* **139,** 830–837
28. Hepojoki, J., Strandin, T., Vaheri, A., and Lankinen, H. (2010) Interactions and oligomerization of hantavirus glycoproteins. *J. Virol.* **84,** 227–242
29. Petäjä-Repo, U. E., Hogue, M., Bhalla, S., Laperrière, A., Morello, J. P., and Bouvier, M. (2002) Ligands act as pharmacological chaperones and increase the efficiency of delta opioid receptor maturation. *EMBO J.* **21,** 1628–1637
30. Chen, J. G., Liu-Chen, S., and Rudnick, G. (1997) External cysteine residues in the serotonin transporter. *Biochemistry* **36,** 1479–1486
31. Chen, R., Wei, H., Hill, E. R., Chen, L., Jiang, L., Han, D. D., and Gu, H. H. (2007) Direct evidence that two cysteines in the dopamine transporter form a disulfide bond. *Mol. Cell Biochem.* **298,** 41–48
32. Forlani, G., Bossi, E., Ghirardelli, R., Giovannardi, S., Binda, F., Bonadiman, L., Ielmini, L., and Peres, A. (2001) Mutation K448E in the external loop 5 of rat GABA transporter rGAT1 induces pH sensitivity and alters substrate interactions. *J. Physiol.* **536,** 479–494
33. Grossman, T. R., and Nelson, N. (2003) Effect of sodium lithium and proton concentrations on the electrophysiological properties of the four mouse GABA transporters expressed in *Xenopus* oocytes. *Neurochem. Int.* **43,** 431–443
34. Lynch, J. W., Jacques, P., Pierce, K. D., and Schofield, P. R. (1998) Zinc potentiation of the glycine receptor chloride channel is mediated by allosteric pathways. *J. Neurochem.* **71,** 2159–2168
35. Hirzel, K., Müller, U., Latal, A. T., Hülsmann, S., Grudzinska, J., Seeliger, M. W., Betz, H., and Laube, B. (2006) Hyperekplexia phenotype of glycine receptor α1 subunit mutant mice identifies Zn^{2+} as an essential endogenous modulator of glycinergic neurotransmission. *Neuron* **52,** 679–690
36. Tóth, K. (2011) Zinc in neurotransmission. *Annu. Rev. Nutr.* **31,** 139–153
37. Laube, B. (2002) Potentiation of inhibitory glycinergic neurotransmission by Zn^{2+}. A synergistic interplay between presynaptic $P2X_2$ and postsynaptic glycine receptors. *Eur. J. Neurosci.* **16,** 1025–1036
38. Ju, P., Aubrey, K. R., and Vandenberg, R. J. (2004) Zn^{2+} inhibits glycine transport by glycine transporter subtype 1b. *J. Biol. Chem.* **279,** 22983–22991
39. Chu, X. P., Wemmie, J. A., Wang, W. Z., Zhu, X. M., Saugstad, J. A., Price, M. P., Simon, R. P., and Xiong, Z. G. (2004) Subunit-dependent high-affinity zinc inhibition of acid-sensing ion channels. *J. Neurosci.* **24,** 8678–8689
40. Baron, A., Voilley, N., Lazdunski, M., and Lingueglia, E. (2008) Acid sensing ion channels in dorsal spinal cord neurons. *J. Neurosci.* **28,** 1498–1508
41. Chen, J., Myerburg, M. M., Passero, C. J., Winarski, K. L., and Sheng, S. (2011) External Cu^{2+} inhibits human epithelial Na^+ channels by binding at a subunit interface of extracellular domains. *J. Biol. Chem.* **286,** 27436–27446
42. Dudev, T., and Lim, C. (2002) Factors governing the protonation state of cysteines in proteins. An *ab initio*/CDM study. *J. Am. Chem. Soc.* **124,** 6759–6766
43. Leskelä, T. T., Markkanen, P. M., Alahuhta, I. A., Tuusa, J. T., and Petäjä-Repo, U. E. (2009) Phe27Cys polymorphism alters the maturation and subcellular localization of the human delta opioid receptor. *Traffic* **10,** 116–129
44. Schülein, R., Zühlke, K., Krause, G., and Rosenthal, W. (2001) Functional rescue of the nephrogenic diabetes insipidus-causing vasopressin V2 receptor mutants G185C and R202C by a second site suppressor mutation. *J. Biol. Chem.* **276,** 8384–8392
45. Williams, S. E., Reed, A. A., Galvanovskis, J., Antignac, C., Goodship, T., Karet, F. E., Kotanko, P., Lhotta, K., Morinière, V., Williams, P., Wong, W., Rorsman, P., and Thakker, R. V. (2009) Uromodulin mutations causing familial juvenile hyperuricaemic nephropathy lead to protein maturation defects and retention in the endoplasmic reticulum. *Hum. Mol. Genet.* **18,** 2963–2974
46. Krishnamurthy, H., and Gouaux, E. (2012) X-ray structures of LeuT in substrate-free outward-open and apo inward-open states. *Nature* **481,** 469–474

47. Bartholomäus, I., Milan-Lobo, L., Nicke, A., Dutertre, S., Hastrup, H., Jha, A., Gether, U., Sitte, H. H., Betz, H., and Eulenburg, V. (2008) Glycine transporter dimers. Evidence for occurrence in the plasma membrane. *J. Biol. Chem.* **283,** 10978–10991
48. Pace, C. N., Grimsley, G. R., and Scholtz, J. M. (2009) Protein ionizable groups. pK values and their contribution to protein stability and solubility. *J. Biol. Chem.* **284,** 13285–13289
49. Chen, Z., Dillon, G. H., and Huang, R. (2004) Molecular determinants of proton modulation of glycine receptors. *J. Biol. Chem.* **279,** 876–883
50. Aubrey, K. R., Mitrovic, A. D., and Vandenberg, R. J. (2000) Molecular basis for proton regulation of glycine transport by glycine transporter subtype 1b. *Mol. Pharmacol.* **58,** 129–135
51. Krishtal, O. (2003) The ASICs. Signaling molecules? Modulators? *Trends Neurosci.* **26,** 477–483
52. Jasti, J., Furukawa, H., Gonzales, E. B., and Gouaux, E. (2007) Structure of acid-sensing ion channel 1 at 1.9 Å resolution and low pH. *Nature* **449,** 316–323
53. Krishtal, O. A., Osipchuk, Y. V., Shelest, T. N., and Smirnoff, S. V. (1987) Rapid extracellular pH transients related to synaptic transmission in rat hippocampal slices. *Brain Res.* **436,** 352–356
54. Li, Y. F., Wu, L. J., Li, Y., Xu, L., and Xu, T. L. (2003) Mechanisms of H^+ modulation of glycinergic response in rat sacral dorsal commissural neurons. *J. Physiol.* **552,** 73–87
55. Smart, T. G., Hosie, A. M., and Miller, P. S. (2004) Zn^{2+} ions. Modulators of excitatory and inhibitory synaptic activity. *Neuroscientist* **10,** 432–442